Cell Reports

Article

A Family of T6SS Antibacterial Effectors Related to L,D-Transpeptidases Targets the Peptidoglycan

Graphical Abstract

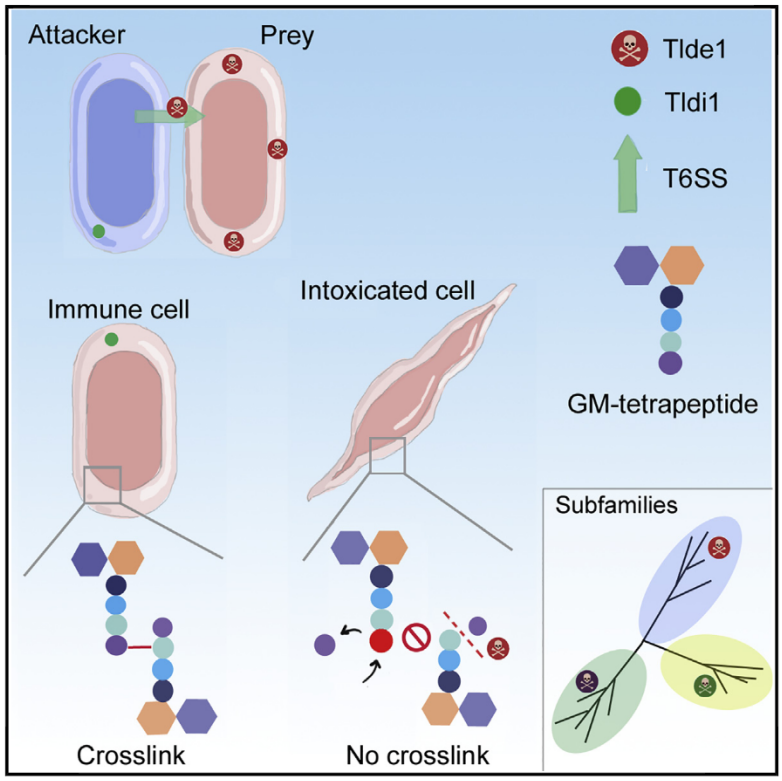

Authors

Stephanie Sibinelli-Sousa, Julia T. Hespanhol, Gianlucca G. Nicastro, ..., Robson F. de Souza, Cristiane R. Guzzo, Ethel Bayer-Santos

Correspondence

ebayersantos@usp.br

In Brief

Antibacterial toxic effectors are an armory used by bacteria to compete against rivals. Sibinelli-Sousa et al. reveal the mechanism by which a family of T6SS effectors interferes with target bacteria peptidoglycan. Tlde1 cleaves and modifies peptide stem precursors and reduces their availability, preventing peptidoglycan synthesis.

Highlights

- Tlde1 is an antibacterial T6SS effector related to L,D-transpeptidases
- Tlde1 does not form crosslinks between peptide stems
- Tlde1 has L,D-carboxypeptidase and L,D-transpeptidase exchange activity
- Tlde1 reduces the availability of peptidoglycan precursors and impairs synthesis

Sibinelli-Sousa et al., 2020, Cell Reports *31*, 107813
June 23, 2020
https://doi.org/10.1016/j.celrep.2020.107813

CellPress

Cell Reports

CellPress
OPEN ACCESS

Article

A Family of T6SS Antibacterial Effectors Related to L,D-Transpeptidases Targets the Peptidoglycan

Stephanie Sibinelli-Sousa,[1,4] Julia T. Hespanhol,[1,4] Gianlucca G. Nicastro,[1] Bruno Y. Matsuyama,[2] Stephane Mesnage,[3] Ankur Patel,[3] Robson F. de Souza,[1] Cristiane R. Guzzo,[1] and Ethel Bayer-Santos[1,5,*]

[1]Departamento de Microbiologia, Instituto de Ciências Biomédicas, Universidade de São Paulo, São Paulo 05508-900, Brazil
[2]Departamento de Bioquímica, Instituto de Química, Universidade de São Paulo, São Paulo 05508-000, Brazil
[3]Department of Molecular Biology and Biotechnology, University of Sheffield, Sheffield S10 2TN, UK
[4]These authors contributed equally
[5]Lead Contact
*Correspondence: ebayersantos@usp.br
https://doi.org/10.1016/j.celrep.2020.107813

SUMMARY

Type VI secretion systems (T6SSs) are nanomachines used by bacteria to inject toxic effectors into competitors. The identity and mechanism of many effectors remain unknown. We characterized a *Salmonella* T6SS antibacterial effector called Tlde1 that is toxic in target-cell periplasm and is neutralized by its cognate immunity protein (Tldi1). Microscopy analysis reveals that cells expressing Tlde1 stop dividing and lose cell envelope integrity. Bioinformatic analysis uncovers similarities between Tlde1 and the catalytic domain of L,D-transpeptidases. Point mutations on conserved catalytic residues abrogate toxicity. Biochemical assays reveal that Tlde1 displays both L,D-carboxypeptidase activity by cleaving peptidoglycan tetrapeptides between *meso*-diaminopimelic acid[3] and D-alanine[4] and L,D-transpeptidase exchange activity by replacing D-alanine[4] by a non-canonical D-amino acid. Phylogenetic analysis shows that Tlde1 homologs constitute a family of T6SS-associated effectors broadly distributed among Proteobacteria. This work expands our current knowledge about bacterial effectors used in interbacterial competition and reveals a different mechanism of bacterial antagonism.

INTRODUCTION

Bacteria commonly live in densely populated polymicrobial communities and compete over scarce resources. Several types of contact-dependent antagonistic interactions between bacteria have been described (García-Bayona and Comstock, 2018). The type VI secretion system (T6SS) is a dynamic contractile structure evolutionarily related to bacteriophage tails that delivers protein effectors in a contact-dependent manner into diverse cellular types, including eukaryotic host cells and rival bacteria and fungi (Hachani et al., 2016; Coulthurst, 2019; Trunk et al., 2019). T6SSs were also reported to display contact-independent functions in which secreted effectors facilitate the scavenging of scarce metal ions (Wang et al., 2015; Si et al., 2017a, 2017b; DeShazer, 2019).

The T6SS is anchored in the bacterial envelope and is composed of 13 core structural components that assemble into 3 major complexes: the trans-membrane complex, the baseplate, and the tail (Nguyen et al., 2018). A conformational change in the T6SS baseplate is thought to trigger the contraction of a cytoplasmic sheath, expelling a spear-like structure to puncture target cell membranes (Wang et al., 2017; Salih et al., 2018). The spear is composed of Hcp (hemolysin co-regulated protein) hexamers capped with a trimer of VgrG (valine-glycine repeat protein G) proteins and a PAAR (proline-alanine-alanine-arginine) protein tip (Mougous et al., 2006; Renault et al., 2018; Shneider et al., 2013). Cargo effector proteins associate through non-covalent interactions with these structural components, while specialized effectors are presented as additional C-terminal domains fused to Hcp, VgrG, or PAAR proteins (Cianfanelli et al., 2016; Jana and Salomon, 2019). Consequently, along with the Hcp-VgrG-PAAR puncturing device, a cocktail of effectors is delivered into the target cell after each contraction event.

Antibacterial effectors delivered by the T6SS induce toxicity by targeting important structural components or affecting target-cell metabolism. Several families of effectors have been described, including peptidoglycan amidases and hydrolases, phospholipases, nucleases, nicotinamide adenine dinucleotide (phosphate) (NAD(P)+)-glycohydrolases, pore-forming proteins, and enzymes that synthesize (p)ppApp (Russell et al., 2011, 2012; Koskiniemi et al., 2013; Whitney et al., 2013; Ma et al., 2014; Altindis et al., 2015; Tang et al., 2018; Ahmad et al., 2019; Jana et al., 2019; Mariano et al., 2019; Wood et al., 2019). An example of an effector inducing toxicity by posttranslational modification (ADP-ribosylation) of the cytoskeleton component FtsZ has also been reported (Ting et al., 2018). To prevent self-intoxication, bacteria have a specific immunity protein for each antibacterial T6SS effector. Immunity proteins are encoded adjacent to their cognate effector, reside in the same cellular compartment where the effector exerts its toxic effect,

and typically work by binding directly to the effector (Hood et al., 2010; Russell et al., 2012).

The peptidoglycan sacculus maintains cell shape and provides mechanical strength to resist osmotic pressure (Vollmer et al., 2008). The mesh-like structure surrounds the cytoplasm and inner membrane and is composed of glycan chains of alternating *N*-acetylglucosamine (NAG) and *N*-acetylmuramic acid (NAM) residues crosslinked by short peptides containing both L- and D-amino acids. In Gram-negative bacteria, the peptide component is usually made of the following amino acids: L-alanine[1], D-*iso*glutamic acid[2] (D-*i*Glu), *meso*-diaminopimelic acid[3] (*m*DAP), D-alanine[4], and D-alanine[5] (Typas et al., 2011). Peptide stems are crosslinked to one another by transpeptidases (TPases) that could be either D,D-TPases, forming crosslinks between the D-Ala[4] of a pentapeptide donor stem and the *m*DAP[3] of a tetrapeptide acceptor stem (4 → 3 crosslink), or L,D-TPases, forming crosslinks between the *m*DAP[3] of one tetrapeptide and the *m*DAP[3] of another tetrapeptide (3 → 3 crosslink) (Vollmer and Bertsche, 2008). D,D-TPases (also called penicillin-binding proteins [PBPs]) are the primary enzymes performing crosslinks in the peptidoglycan and are inhibited by β-lactam antibiotics, which mimic the terminal D-Ala[4]-D-Ala[5] moiety of the donor pentapeptide (King et al., 2016).

T6SS effectors targeting the peptidoglycan distribute into 2 groups: (1) those that act as amidases and cleave within the peptide stems or crosslinks (Russell et al., 2012) and (2) those that act as glycoside hydrolases and cleave the glycan backbone (Whitney et al., 2013). T6SS amidase effectors form 4 phylogenetically distinct families called Tae1–Tae4 (type VI amidase effectors), and the preferred cleavage site within the peptidoglycan varies between each family (Russell et al., 2012). Tae1 and Tae4 cleave between D-*i*Glu[2] and *m*DAP[3] within the same peptide stem, while Tae2 and Tae3 cleave the crosslink bridge between D-Ala[4] and *m*DAP[3] of different peptide stems (Russell et al., 2012). An additional effector called TaeX cleaves between NAM glycan and the first L-Ala[1] of the peptide stem (Ma et al., 2018). The superfamily of T6SS glycoside hydrolases was divided into 3 families called Tge1–Tge3 (type VI glycoside hydrolase effector) (Whitney et al., 2013). Tge members have a lysozyme-like fold and were shown to cleave the glycoside bond between NAM and NAG (Whitney et al., 2013).

In *Salmonella enterica,* T6SS gene clusters are encoded within different pathogenicity islands (SPIs), depending on the subspecies and serovar (Blondel et al., 2009; Bao et al., 2019). *S. enterica* subsp. *enterica* serovar Typhimurium (*S.* Typhimurium) encodes only one T6SS that is located within SPI-6. The expression of SPI-6 T6SS genes is not detected under laboratory culture conditions, but it is activated in later stages of macrophage infection (Parsons and Heffron, 2005; Mulder et al., 2012) and in the mammalian gut, where it works as an antibacterial weapon to kill the resident species of the microbiota, contributing to *Salmonella* colonization (Sana et al., 2016). The histone-like nucleoid structuring protein (H-NS) (Brunet et al., 2015) and the ferric uptake regulator (Fur) (Wang et al., 2019) were reported to repress SPI-6 T6SS genes *in vitro*. Only one effector (Tae4) has been described to date as a substrate for SPI-6 T6SS. Tae4 is an antibacterial effector and works as an L,D-endopeptidase cleaving between D-*i*Glu[2] and *m*DAP[3] (Russell et al., 2012; Benz et al., 2013; Zhang et al., 2013).

Here, we set out to identify new SPI-6 T6SS effectors and report the characterization of a family of antibacterial effectors containing the domain of unknown function DUF2778, which displays both L,D-carboxypeptidase (CPase) and L,D-TPase exchange activities. This family is evolutionarily related to enzymes that have an L,D-TPase fold and is broadly distributed among α-, β-, and γ-Proteobacteria. We also describe a protein containing DUF2195 as the immunity protein (Tldi1). Expression of Tlde1 in the periplasm of target *Escherichia coli* prevents cell division and induces cell elongation, swelling, and lysis. Our study reveals a different mechanism for effector-mediated bacterial antagonism and indicates that Tlde1 targets the peptidoglycan synthesis in two ways: (1) the L,D-CPase activity reduces the amount of acceptor tetrapeptide stems, thus reducing the formation of new crosslinks by D,D-TPases; and (2) the L,D-TPase exchange activity promotes the incorporation of non-canonical D-amino acid (NCDAA) into tetrapeptides affecting their recycling and reducing the availability of cell wall precursors and substrates for D,D-transpeptidation. These activities together result in an altered formation of the division septum and an overall weakened peptidoglycan structure.

RESULTS

Tlde1-Tldi1 Are an Antibacterial Effector-Immunity Pair

To search for new T6SS effectors secreted by *S.* Typhimurium, we inspected the SPI-6 T6SS gene cluster of the 14028s strain looking for bicistrons that could resemble an antibacterial effector-immunity pair (Figure 1A). The gene annotated as *STM14_0336* (Tlde1) encodes a small protein of 173 amino acids and contains a DUF2778 (PF10908). Upstream to this gene, there is another small protein (138 amino acids) containing a DUF2195 annotated as *STM14_0335* (Tldi1), which encodes a predicted Sec signal peptide sequence for periplasmic localization (Figure S1A) (Almagro Armenteros et al., 2019). Bastion6 software prediction (Wang et al., 2018) indicates that STM14_0336 could be a T6SS effector (score 0.758). To test whether STM14_0336 and STM14_0335 are a bona fide effector-immunity pair, we cloned these genes into compatible vectors under the control of different promoters. To evaluate the toxicity of STM14_0336 upon expression in *E. coli* and to establish in which cellular compartment the toxin exerts its effect, *STM14_0336* was cloned into the pBRA vector under the control of the P_{BAD} promoter (inducible by L-arabinose and repressed by D-glucose), both with and without an N-terminal PelB periplasmic localization sequence (pBRA SP-Tlde1 or pBRA Tlde1). The putative STM14_0335 immunity protein was cloned with its endogenous signal peptide into the pEXT22 vector under the control of the P_{TAC} promoter, which can be induced by isopropyl β-D-1-thiogalactopyranoside (IPTG) (pEXT22 Tldi1). *E. coli* strains carrying different combinations of pBRA and pEXT22 plasmids were serially diluted and incubated on LB agar containing either 0.2% D-glucose or 0.2% L-arabinose plus 200 μM IPTG (Figure 1B). Results showed that STM14_0336 is toxic when directed to the periplasm of *E. coli* (pBRA SP-Tlde1) but not to the cytoplasm (pBRA Tlde1), and that STM14_0335 (pEXT22 Tldi1) could neutralize its toxicity (Figure 1B). To confirm

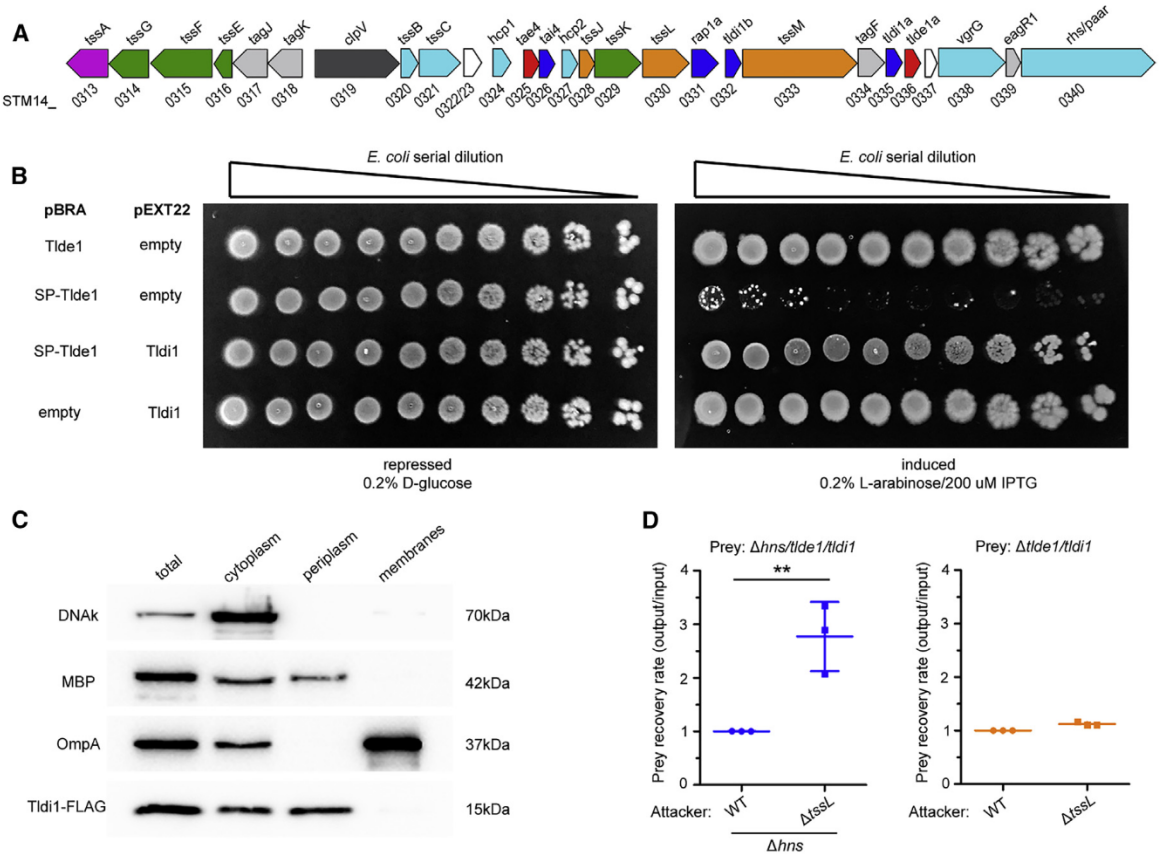

Figure 1. Tlde1/Tldi1 Are an Antibacterial Effector-Immunity Pair

(A) Schematic representation of SPI-6 T6SS gene cluster of *S.* Typhimurium 14028s: membrane complex (orange), baseplate (green), tail (light blue), toxins (red), immunity proteins (dark blue), chaperone and stabilizing protein (pink), ATPase for disassembly (dark gray), and accessory proteins (light gray). Accession numbers are indicated below.

(B) The 4-fold dilutions of *E. coli* containing pBRA and pEXT22 constructs, as indicated, spotted onto LB agar plates. Growth inhibition is observed upon expression of the SP-Tlde1 construct and can be neutralized by co-expression of Tldi1.

(C) *E. coli* cells expressing pEXT22 Tldi1-FLAG were fractionated and analyzed by western blot using anti-FLAG, anti-DNAk (cytoplasmic), anti-OmpA (membranes), and anti-MBP (periplasm) antibodies.

(D) Bacterial competition assay using *S.* Typhimurium LT2 strain (WT, Δ*tssL*, and Δ*tlde1/tldi1*) either in the Δ*hns* (activated T6SS) or the WT background (repressed T6SS). The prey recovery rate was calculated by dividing the colony-forming unit (CFU) counts of the output by the input. Data represent the mean ± SD of 3 independent experiments performed in triplicate and were analyzed through comparison with WT that were normalized to 1. $^{**}p < 0.01$ (Student's t test). See also Figure S1.

the subcellular localization of the immunity protein, *E. coli* cells expressing a C-terminal FLAG-tagged version of Tldi1 were subjected to subcellular fractionation, and results confirmed its periplasmic localization (Figure 1C). Western blot signals detected with anti-FLAG and anti-maltose-binding protein (MBP) in the cytoplasmic fraction represent a portion of soluble periplasmic proteins that were not completely extracted during the osmotic shock (Figure 1C).

The SPI-6 T6SS of *S.* Typhimurium is repressed in LB media by the silencer protein H-NS, and its deletion activates the T6SS (Brunet et al., 2015). After analyzing published RNA sequencing (RNA-seq) data comparing wild-type (WT) and Δ*hns* strains (LT2 strain background) (Navarre et al., 2006), we confirmed that VgrG/STM0289 and Tae4/STM0277 mRNA levels were upregulated by 7.2-fold and 4.6-fold, respectively, in Δ*hns* compared to WT. The same pattern was observed for Tlde1/STM0288, which was upregulated by 3.5-fold in Δ*hns* compared to WT. To analyze whether Tlde1 is a T6SS substrate, we performed interbacterial competition assays using WT and Δ*tssL* (attacker) versus a mutant strain lacking the effector-immunity pair Δ*tlde1/tldi1* (prey), either in the Δ*hns* (activated T6SS) or the WT background (repressed T6SS). Results showed that the prey recovery rate was ~3-fold higher in Δ*tssL*/Δ*hns* compared to Δ*hns*, while no difference was observed when the T6SS was repressed (Figure 1D). These results confirm that Tlde1 is an antibacterial effector secreted via the SPI-6 T6SS.

Tlde1 Intoxication Causes Altered Cell Division, Swelling, and Lysis

To gather further insight on the mechanism by which Tlde1 induces toxicity, we performed time-lapse microscopy to evaluate the growth and morphology of individual *E. coli* cells carrying

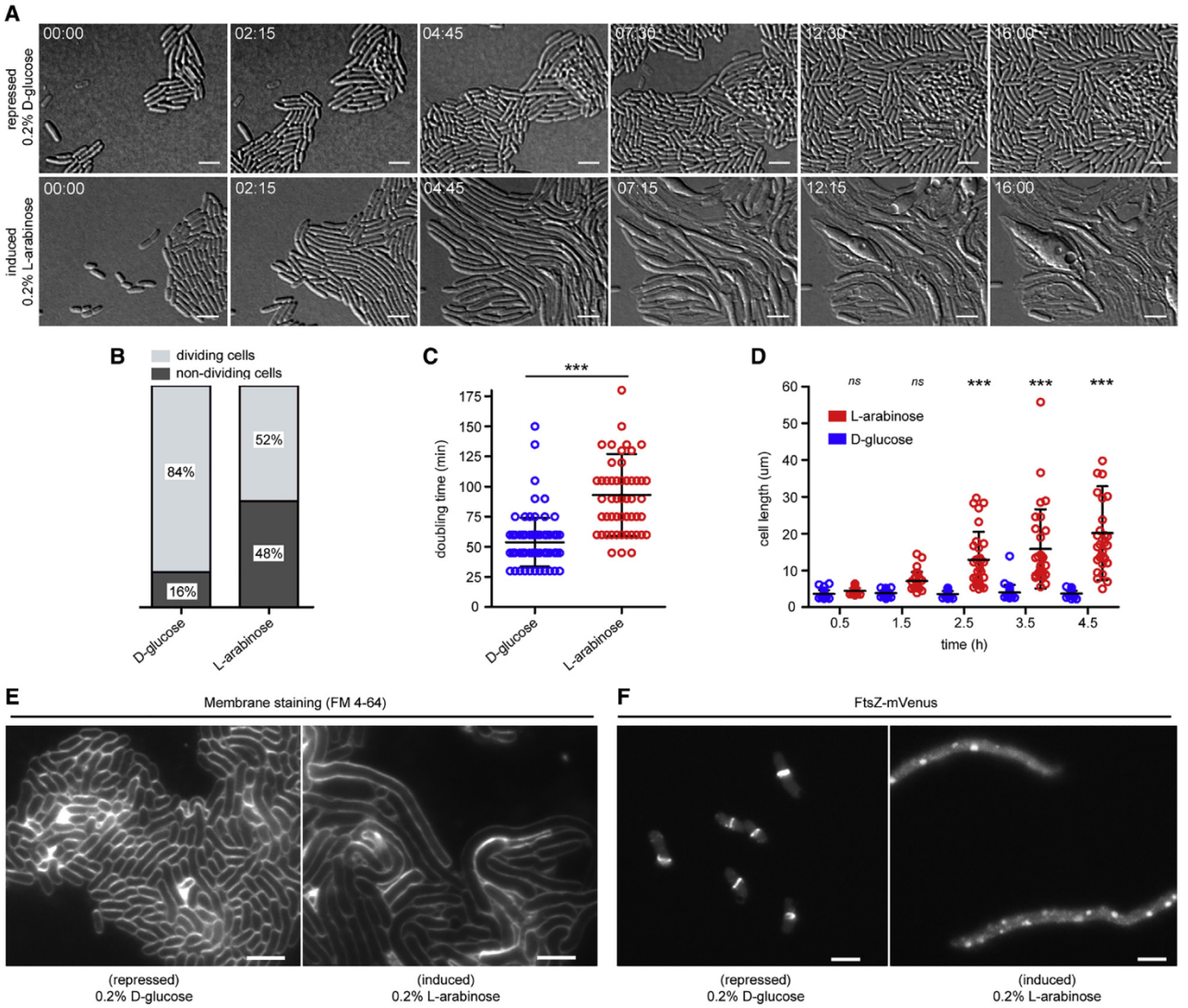

Figure 2. Tlde1 Is a Periplasmic-Acting Toxin That Alters Cell Division and Weakens the Peptidoglycan

(A) Time-lapse microscopy of *E. coli* cells expressing SP-Tlde1 grown on LB agar pads containing either 0.2% D-glucose (repressed) or 0.2% L-arabinose (induced). Scale bar, 5 μm. Timestamps in hours:minutes.

(B) Percentage of dividing and non-dividing cells observed in (A) between 0 and 4.5 h.

(C) Doubling time in minutes of cells that divided quantified in (B); error bars represent the SDs of the means of ~100 cells in each condition. ***$p < 0.0001$ (Student's t test).

(D) Cell length of cells observed in (A) between 0 and 4.5 h; error bars represent the SDs of the means of ~30 cells measured at each time point, and were analyzed through comparison with D-glucose at 0.5 h by 1-way ANOVA followed by Dunnett's multiple comparison test. ***$p < 0.0001$ and ns, not significant.

(E) Fluorescence microscopy images of *E. coli* cells harboring pBRA SP-Tlde1 labeled with the membrane dye FM 4-64 and incubated with 0.2% D-glucose (repressed) or 0.2% L-arabinose (induced). Scale bar, 5 μm.

(F) Fluorescence microscopy images of *E. coli* FtsZ-mVenus carrying pBRA SP-Tlde1 incubated with 0.2% D-glucose (repressed) or 0.2% L-arabinose (induced). Scale bar, 5 μm.

pBRA SP-Tlde1. *E. coli* cells grew normally when incubated on LB agar pads containing 0.2% D-glucose (repressed) over a time frame of 16 h (Figure 2A; Video S1). However, incubation in the presence of 0.2% L-arabinose induced a series of alterations in cell division and morphology (Figures 2A–2F; Video S2). At early time points (up to 4.5 h) after induction with L-arabinose, intoxicated cells tend to stop dividing or divide with increased doubling times (Figures 2B and 2C). Between 0 and 4.5 h of incubation in L-arabinose, only 52% of intoxicated cells were observed to undergo at least 1 round of cell division, with a doubling time of 93 ± 34 min, while 84% of cells grown with D-glucose divided in the same time frame, with a doubling time of 54 ± 20 min (Figures 2B and 2C). Although intoxicated cells had clearly impaired cell division, they continued to increase in

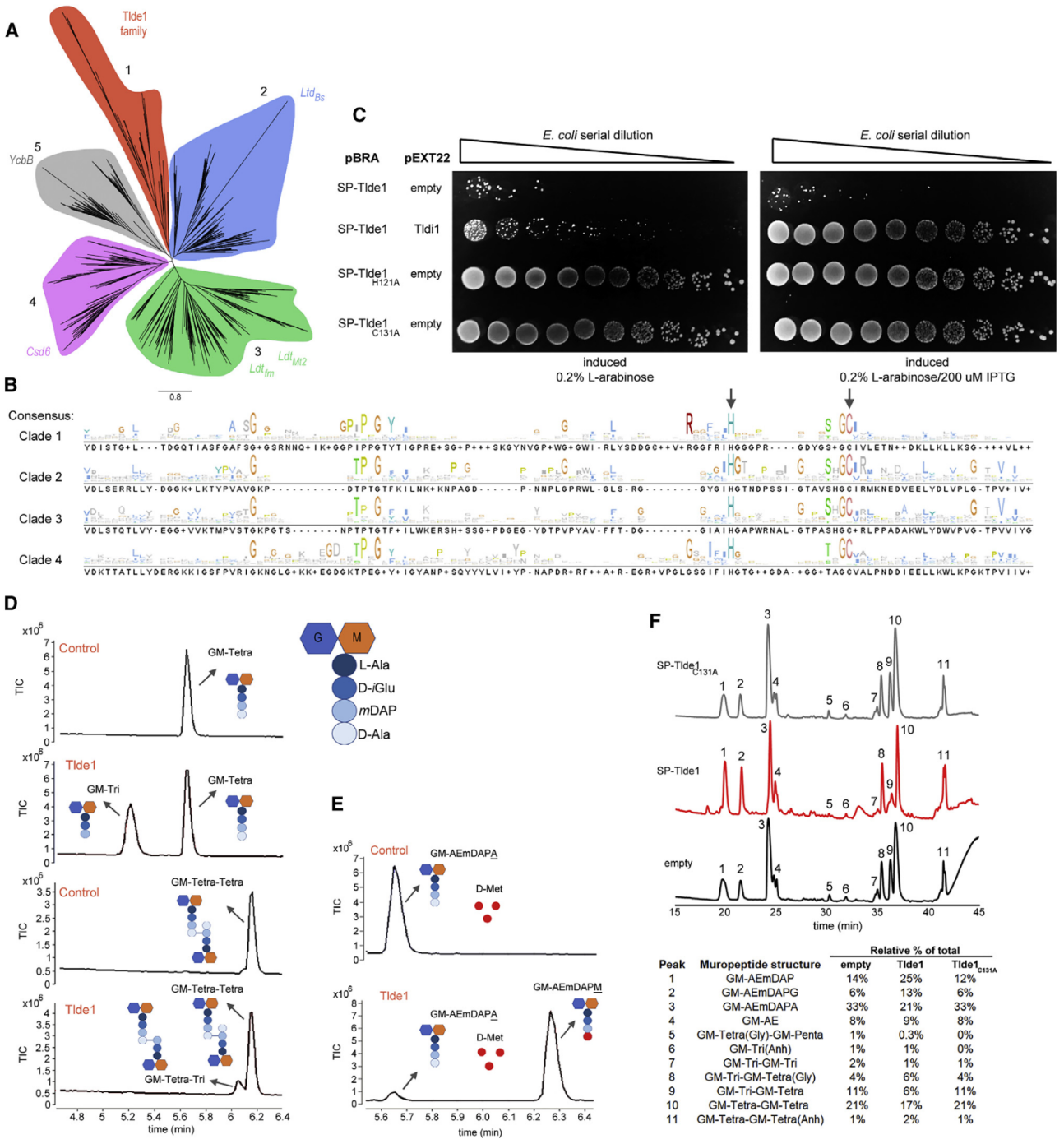

Peak	Muropeptide structure	Relative % of total empty	Tlde1	Tlde1 C131A
1	GM-AEmDAP	14%	25%	12%
2	GM-AEmDAPG	6%	13%	6%
3	GM-AEmDAPA	33%	21%	33%
4	GM-AE	8%	9%	8%
5	GM-Tetra(Gly)-GM-Penta	1%	0.3%	0%
6	GM-Tri(Anh)	1%	1%	0%
7	GM-Tri-GM-Tri	2%	1%	1%
8	GM-Tri-GM-Tetra(Gly)	4%	6%	4%
9	GM-Tri-GM-Tetra	11%	6%	11%
10	GM-Tetra-GM-Tetra	21%	17%	21%
11	GM-Tetra-GM-Tetra(Anh)	1%	2%	1%

Figure 3. Tlde1 Is Evolutionarily Related to L,D-Transpeptidases

(A) Maximum likelihood phylogenetic tree of Tlde1 (DUF2778) homologs identified using JackHMMER and HMMsearch. Tlde1 is a distant homolog of L,D-TPases with the YkuD domain (PF03734). DUF2778-containing proteins grouped separately (clade 1, red) from known L,D-TPases.

(B) Partial amino acid sequence alignment of consensus sequences from clades 1–4. Arrows indicate conserved catalytic histidine and cysteine residues of L,D-TPases.

(C) The 4-fold dilutions of *E. coli* containing pBRA and pEXT22 constructs, as indicated, spotted onto LB agar plates. Growth inhibition is observed upon the expression of SP-Tlde1, but toxicity is abolished by H_{121}A and C_{131}A point mutations.

(D) Reversed phase-HPLC (RP-HPLC) coupled to MS showing purified monomeric GM-tetrapeptides or dimeric GM-tetrapeptide-GM-tetrapeptide incubated with recombinant Tlde1. The schematic structure of a muropeptide is shown. L-Ala, L-alanine; D-*i*Glu, D-*iso*glutamic acid; *m*DAP, *meso*-diaminopimelic acid; D-Ala, D-alanine; G, *N*-acetylglucosamine; M, *N*-acetylmuramic acid.

(legend continued on next page)

size (Figure 2D; Video S2). After 4.5 h, cells grown in L-arabinose had an average cell length of 20 ± 12 μm, while cells grown in D-glucose displayed an average length of 3.7 ± 0.7 μm (Figure 2D). To analyze whether intoxicated cells were not dividing or dividing but not segregating into daughter cells, we incubated *E. coli* with the membrane dye FM 4-64 (Figure 2E). Results showed that elongated cells lack membrane invaginations indicative of a division septum (Figure 2E). Transformation of an *E. coli* strain in which mVenus was fused to the endogenous *ftsZ* gene (Moore et al., 2016) with our pBRA SP-Tlde1 plasmid showed that the FtsZ-mVenus localization pattern was altered in intoxicated cells (Figure 2F). It is unclear at this point whether the Z-ring assembly was affected by the Tlde1 activity or is an indirect result of a pleiotropic effect such as the loss of membrane potential.

After 4.5 h in L-arabinose, *E. coli* pBRA SP-Tlde1 cells tend to swell and burst, indicating that the integrity of their peptidoglycan structure was compromised (Figure 2A; Video S2). No obvious alterations were observed in *E. coli* pBRA SP-Tlde1 cells grown in the presence of D-glucose during the same time frame (Figure 2A; Video S1).

Tlde1 Is Evolutionarily Related to L,D-Transpeptidases

To gain insight into the molecular function of Tlde1, we used its amino acid sequence as a query in JackHMMER searches (Potter et al., 2018) to fetch a total of 143,242 sequences with significant similarity (inclusion threshold $\leq 10^{-3}$ and e-value $\leq 10^{-6}$) from the NCBI nr database (June 7, 2019). Additional JackHMMER searches using selected hits of the first iterative search as queries and the Pfam models DUF2778 (PF10908), YkuD (PF03734), and YkuD_2 (PF13645) resulted in a total of 153,327 sequences. To reduce data complexity, we clustered amino acid sequences requiring 80% coverage for all pairwise alignments generated by MMseqs (Steinegger and Söding, 2017), and a maximum e-value of 10^{-3}, resulting in 4,113 groups. A single amino acid sequence was chosen as representative from each group with at least 9 members, resulting in 943 sequences representing a sample of 145,969 homologs. These representative sequences were used to build a phylogenetic tree using the maximum likelihood method (Figure 3A). The homologs of Tlde1 clustered into 5 main clades: clade 1 (red, 6,332 sequences), to which Tlde1 belongs, is composed of proteins containing the uncharacterized DUF2778 domain (Tlde1 family); clade 2 (blue, 44,540 sequences) contains the L,D-TPases from *Bacillus subtilis* (Ldt_{Bs}, PDB: 1Y7M) (Bielnicki et al., 2006); clade 3 (green, 44,090 sequences) contains L,D-TPases from *Enterococcus faecium* (Ldt_{fm}, PDB: 1ZAT) (Biarrotte-Sorin et al., 2006), *Mycobacterium abscessus* (Ldt_{Mab}, PDB: 5UWV) (Kumar et al., 2017), and *Mycobacterium tuberculosis* (Ldt_{Mt1-3}, PDB: 3TUR, 5DCC) (Erdemli et al., 2012; Bianchet et al., 2017); clade 4 (purple, 25,242 sequences) contains an enzyme from *Helicobacter pylori* (Csd6, PDB: 4XZZ) that has a catalytic domain resembling L,D-TPases but with L,D-CPase activity (Kim et al., 2015); and clade 5 (gray, 25,765 sequences) contains an L,D-TPase from *E. coli* (YcbB, PDB: 6NTW) (Caveney et al., 2019) and proteins recognized by the Pfam model YkuD_2.

Multiple amino acid sequence alignments of proteins from each clade revealed conserved residues similar to the conserved motif described for L,D-TPases: $\underline{H}XX_{14-17}[S/T]HG\underline{C}h$ (underlined letters are conserved catalytic residues and "h" hydrophobic residues) (Erdemli et al., 2012) (Figure 3B). According to the Pfam hidden Markov model (HMM) logo, the number of residues between the conserved catalytic His and Cys is smaller in DUF2778 (PF10908) compared to YkuD (PF3734). To evaluate whether the conserved His in position 121 and Cys in position 131 of Tlde1 are required to induce toxicity, we produced point mutations by substituting these residues for alanine. Plasmids containing point mutations (pBRA SP-$Tlde1_{H121A}$ and pBRA SP-$Tlde1_{C131A}$) were transformed into *E. coli* cells and grown in the presence of 0.2% L-arabinose, revealing the complete loss of toxicity (Figure 3C).

To determine the enzymatic activity of Tlde1, we incubated purified recombinant protein (Figure S2A) with purified peptidoglycan muropeptides and analyzed the reaction product by reverse-phase high-performance liquid chromatography (HPLC) coupled to mass spectrometry (MS) (Figures 3D and S2B). Results showed that Tlde1 has L,D-CPase activity and cleaves NAG-NAM-tetrapeptides (GM-tetrapeptide) between *m*DAP^3 and D-Ala^4, producing GM-tripeptides (45% of substrate was converted) (Figures 3D). The formation of crosslinked GM-tripeptide-GM-tetrapeptide could not be detected, suggesting that Tlde1 does not have standard L,D-TPase activity (Figure 3D). Crosslinked dimeric GM-tetrapeptide-GM-tetrapeptide forms were also provided as substrates and a small proportion of cleavage was detected between the *m*DAP^3-D-Ala^4 of the acceptor peptide stem during the same incubation period (11% of substrate was cleaved), thus confirming the L,D-CPase activity and suggesting that Tlde1 preferentially uses monomeric GM-tetrapeptide as a substrate (Figure 3D). Also, we could not detect any product indicating that Tlde1 cleaves the D-Ala^4-*m*DAP^3 crosslink bridge between peptide stems (Figure 3D). In addition, co-incubation of GM-tetrapeptides (GM-AE*m*DA$\underline{P}$A) with 1 mM D-methionine and recombinant Tlde1 produced GM-tetrapeptides with D-Met at position 4 (GM-AE*m*DAP$\underline{M}$) (92% of substrate was converted), showing that Tlde1 is able to exchange the last amino acid of GM-tetrapeptides for a NCDAA, as was reported for other L,D-TPases (Figure 3E) (Mainardi et al., 2005).

The composition of peptidoglycan extracted from *E. coli* cells growing at exponential phase is enriched in monomeric GM-tetrapeptides and dimeric GM-tetrapeptide-GM-tetrapeptides (Glauner et al., 1988). During the synthesis of new peptidoglycan, the GM-pentapeptide precursor works as donor peptide stem

(E) RP-HPLC coupled to MS showing purified monomeric GM-tetrapeptides incubated with recombinant Tlde1 and 1 mM D-methionine. Tlde1 shows L,D-TPase exchange activity and incorporation of non-canonical D-amino acid (NCDAA) into peptidoglycan.
(F) RP-HPLC coupled to MS showing total ion chromatograms of muropeptides obtained after mutanolysin digestion of peptidoglycan extracted from *E. coli* harboring empty pBRA (black), pBRA SP-Tlde1 (red), and pBRA SP-$Tlde1_{C131A}$ (gray). Inferred muropeptide structures and relative abundance (relative percentage of total) of each peak was quantified by MassHunter software (bottom).
See also Figure S2.

and is crosslinked to acceptor GM-tetrapeptide stems by the action of D,D-TPases, forming 4 → 3 crosslink bridges (Typas et al., 2011). As Tlde1 turns GM-tetrapeptides into GM-tripeptides *in vitro*, we hypothesized that this activity would promote toxicity *in vivo* by depleting the pool of acceptor GM-tetrapeptides, thus reducing the formation of new crosslinks by endogenous D,D-TPases. To test this hypothesis, we extracted peptidoglycan from *E. coli* cells carrying (1) empty pBRA plasmid, (2) pBRA SP-Tlde1, or (3) pBRA SP-Tlde1$_{C131A}$ incubated with 0.2% L-arabinose for 3 h and analyzed the muropeptides profile by HPLC-MS (Figure 3F). The relative levels of muropeptides in *E. coli* cells expressing SP-Tlde1 were reduced in GM-tetrapeptide (GM-AE*m*DAPA) (21%) compared to cells with empty plasmid (33%) or SP-Tlde1$_{C131A}$ (33%), comprising a 36% reduction in GM-AE*m*DAPA relative levels (Figure 3F). Likewise, the proportion of GM-tripeptides (GM-AE*m*DAP) was enriched in cells expressing SP-Tlde1 (25%) compared to empty and SP-Tlde1$_{C131A}$ (13%), which constitutes a 78% increase in relative levels of GM-tripeptides (Figure 3F). Moreover, the proportion of most crosslinked forms were reduced in *E. coli* cells expressing SP-Tlde1 compared to cells carrying the empty plasmid or expressing SP-Tlde1$_{C131A}$ (Figure 3F). *In vitro* peptidoglycan synthesis assays showed that GM-tripeptides could work as acceptors for D,D-TPases (Born et al., 2006; Bertsche et al., 2005; Catherwood et al., 2020). However, a study of PBP1B TPase showed that the K_m of GM-tripeptides is higher (35 ± 4 μM) than the K_M of GM-tetrapeptides (8.1 ± 0.3 μM), indicating that GM-tripeptides may not be preferential substrates for PBP1B *in vivo* (Catherwood et al., 2020).

Incorporation of NCDAA into peptidoglycan was reported to negatively regulate the amount of peptidoglycan of a given cell and its strength (Lam et al., 2009; Cava et al., 2011). These changes occur mainly because the incorporation of NCDAA into GM-tetrapeptide impairs its recycling, thus leading to reduced amounts of acceptor GM-tetrapeptides and donor GM-pentapeptides for D,D-transpeptidation during peptidoglycan synthesis (Templin et al., 1999; Hernandez et al., 2020). In agreement with the D-amino acid exchange activity detected *in vitro* (Figure 3E), we noticed an increase in GM-AE*m*DAPG (13%) in *E. coli* cells expressing SP-Tlde1 compared to cells with empty plasmid (6%) or catalytic inactive SP-Tlde1$_{C131A}$ (6%), which represents a 116% increase in relative levels (Figure 3F). This result supports the hypothesis that the exchange activity and the incorporation of NCDAA are also relevant *in vivo*. Overall, the combined action of both Tlde1 enzymatic activities impair the peptidoglycan synthesis and its structural strength.

Tlde1 Family Is Widespread among α-, β-, and γ-Proteobacteria

Comprehensive phylogenetic analysis of sequences from clade 1 comprising the Tlde1 family (Figure 3A) showed that proteins segregate into 3 subfamilies (Figure 4A). Given that all subfamilies contain the domain DUF2778, we propose calling them Tlde1a, Tlde1b, and Tlde1c (Figure 4A). The Tlde1a subfamily contains the *S.* Typhimurium Tlde1 effector (Tlde1a^{STM}) and is composed mainly of *S. enterica* subsp. *enterica* serovars encoding SPI-6 T6SS, species of *Bordetella*, and some α-Proteobacteria from Rhizobiaceae and Sphingomonadaceae (Figure 4B; Table S1A). A few examples of *S. enterica* subsp. *diarizonae* (SPI-20 and SPI-21 T6SSs) and *S. enterica* subsp. *salamae* (SPI-19 T6SS) were detected in the Tlde1a subfamily (Figure 4B; Table S1A). In addition, the Tlde1a subfamily also contains examples of Actinobacteria (Streptomycetaceae) and Cyanobacteria (Synechococcaceae, Microcystaceae, Aphanothecaceae); however, it is not clear at this point whether these proteins are secreted by alternative secretion mechanisms, such as the extracellular contractile injection systems (eCIS) (Chen et al., 2019), or simply work in the remodeling of peptidoglycan. The Tlde1b subfamily is abundant in a large variety of species from Enterobacteriaceae, Erwiniaceae, and Yersiniaceae. Examples of *S. enterica* subsp. *arizonae* (SPI-20 and SPI-21 T6SSs) and *S. enterica* subsp. *diarizonae* (SPI-20 and SPI-21 T6SSs) and a few *S. enterica* subsp. *enterica* serovars such as Fresno (SPI-6 T6SS) were detected in the Tlde1b subfamily (Figure 4B; Table S1B). The Tlde1c subfamily is the most widespread and can be found in Enterobacteriaceae, Burkholderiaceae, Pseudomonadaceae, Erwiniaceae, and Yersiniaceae (Figure 4B; Table S1C). Examples of *S. enterica* subsp. *diarizonae* (SPI-20 and SPI-21 T6SSs) and *S. enterica* subsp. *houtenae* (SPI-19 T6SS) were detected in the Tlde1c subfamily.

Examining the genomic context of Tlde1a–Tlde1c members, we observed that at least one member of each subfamily is encoded within a T6SS gene cluster, thus supporting their role as T6SS substrates (Figure 4C; Table S2). In addition, Tlde1b and Tlde1c were found to be associated with orphan Hcp proteins (Figure 4C; Tables S2B and S2C), suggesting that these proteins are secreted as cargo effectors associated with Hcp proteins. Tlde1a members were found outside the T6SS gene cluster together with their putative immunity proteins, although none of these examples were associated with an orphan Hcp (Table S2A). From the total of 1,028 genomes containing a Tlde1a member, 615 (59.8%) are encoded in the vicinity of a T6SS structural gene (Figure 4C). The same high frequency is observed for Tlde1b and Tlde1c subfamilies, with 76.6% (623 of 813) and 42.6% (1,495 of 3,510) of the genomes containing a member in the vicinity of T6SS structural genes, respectively.

Genomic analysis revealed that some organisms encode more than one member of the Tlde1 family (Figures 4C and 4D; Table S1D). *S.* Fresno encodes 2 members within its SPI-6 T6SS, Tlde1a^{SF} (WP_000968384.1) and Tlde1b^{SF} (WP_058115706.1). Tlde1a^{SF} is closely related to *S.* Typhimurium Tlde1a^{STM} (STM14_0336), but the Tlde1b^{SF} homolog is absent in *S.* Typhimurium 14028s (Figure 4C). A close inspection of the *S.* Typhimurium 14028s SPI-6 T6SS locus revealed that it contains an orphan Tldi1b^{STM} immunity protein (STM14_0332) orthologous to *S.* Fresno Tldi1b^{SF} (WP_077921582.1) in the same genomic location (Figures 1A and 4C). This gene is located next to a Tai4 orphan immunity protein (STM14_0331) homologous to Rap1a, which confers immunity to the Tae4 family member Ssp1 from *Serratia marcescens* (English et al., 2012). Growth inhibition assays showed that the Tldi1b^{STM} immunity protein was not able to neutralize the toxicity of Tlde1a^{STM}, thus confirming the specificity of each immunity protein to its effector (Figure S3) and suggesting that Tldi1b^{STM} and Rap1a may play a role in immunity against effectors secreted by other bacteria.

The domain architecture of most Tlde1 members is usually quite simple and composed of a single DUF2778 domain, but

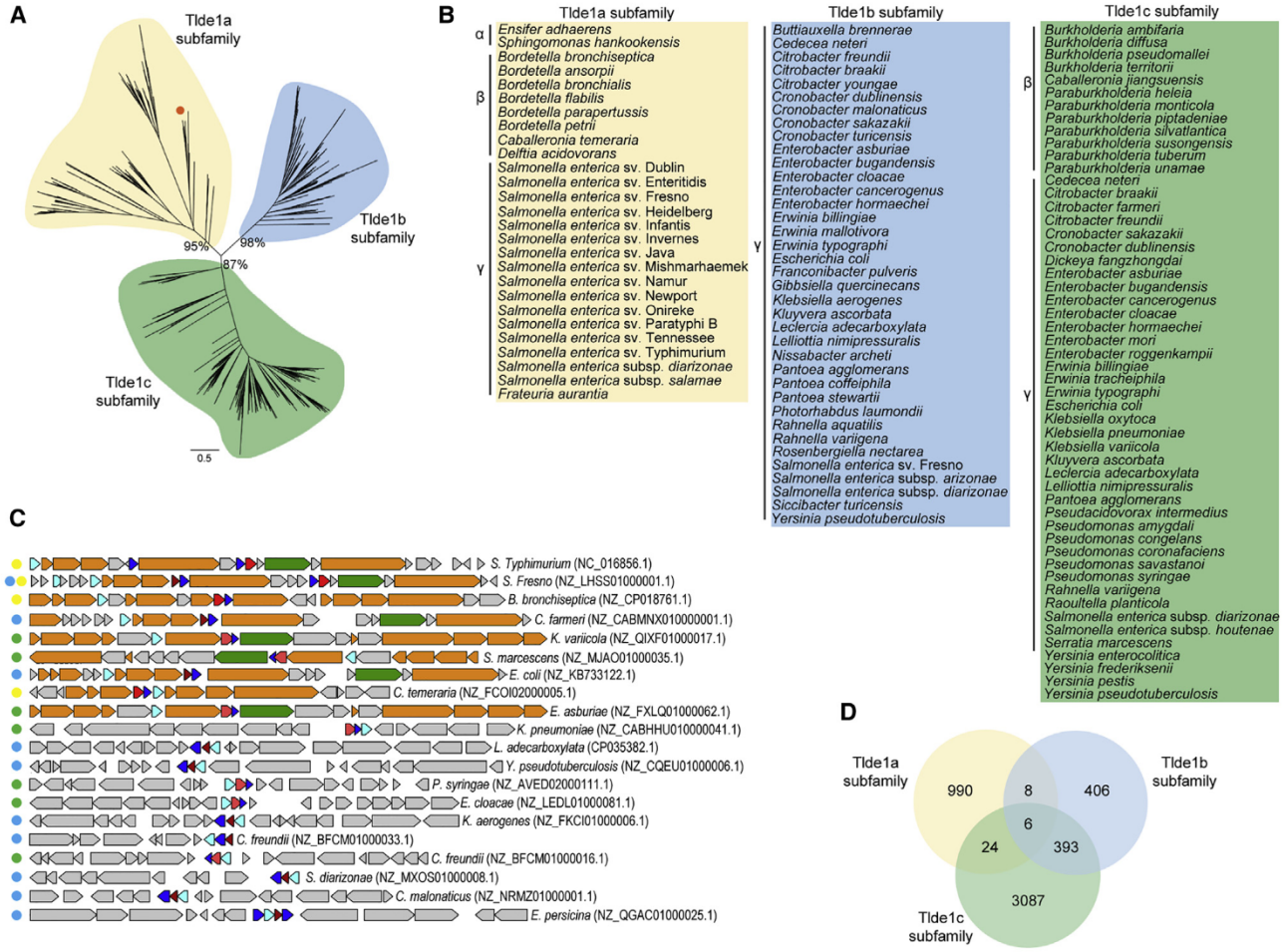

Figure 4. Tlde1 Family Is Widespread in Proteobacteria

(A) Maximum likelihood phylogenetic tree of Tlde1 family (clade 1; Figure 3A), showing its division into 3 subfamilies (Tlde1a, Tlde1b, and Tlde1c). Non-parametric bootstrap values at the branches defining each subfamily are indicated. The position of *S.* Typhimurium Tlde1a is highlighted by an orange dot.

(B) List of common bacterial species encoding members of Tlde1a, Tlde1b, and Tlde1c. The toxic effector is widespread and detected among α-, β-, and γ-Proteobacteria.

(C) Schematic representation of the genomic context of Tlde1a, Tlde1b, and Tlde1c members. T6SS structural genes (orange), VgrG genes (green), Hcp genes (light blue), Tlde1a-c members (red), and their cognate immunity proteins Tldi1a-c (dark blue). Bacterial species and genome accession number are described on the right side of each cluster. Colored dots on the left side denote the subfamily to which the effector belongs: yellow (Tlde1a), blue (Tlde1b), and green (Tlde1c).

(D) Venn diagram representing the total number of bacterial genomes that encode one or more Tlde1a– Tlde1c member.

See also Figure S3 and Tables S1 and S2.

a few examples such as *Shigella sonnei* WP_052983304.1 present DUF2778 at the C-terminal region of rearrangement hotspot (Rhs) proteins, which are encoded close to PAAR-containing proteins that are secreted via T6SS (Koskiniemi et al., 2013). These Rhs-DUF2778 proteins are mainly represented in the Tlde1c subfamily, in which 11% (387 of 3,510) of the genomes display a member fused to Rhs protein (Table S1C). Moreover, DUF2778-containing proteins could be found located in the vicinity of genes encoding other secretion systems such as T1SS (*abc, omf, mfp*), T2SS (*gspD-N*), T4SS (*virb1-10*), and T5SS (PF03797, PF03895, translocator) (Table S2) (Abby et al., 2016), suggesting that these DUF2778-containing proteins may have been recruited to be part of the polymorphic toxin cassettes that are known to be associated with various protein secretion systems (Zhang et al., 2012). These results are in line with bioinformatic analyses that predicted polymorphic toxins with L,D-peptidase domains fused to Rhs repeats or domains related to secretory systems and were linked to the neighboring immunity proteins DUF2750/Imm16 and DUF2750/Imm57 (Zhang et al., 2012).

DISCUSSION

In this study, we identified and characterized a family of T6SS antibacterial effectors, which is evolutionarily related to L,D-TPases containing the YkuD domain (formerly called ErfK/YbiS/YcfS/YnhG). The founding member of this family, Tlde1 from *S.* Typhimurium, displays both L,D-CPase activity, cleaving

peptidoglycan tetrapeptides between *m*DAP[3] and D-Ala[4], and L,D-TPase exchange activity, replacing D-Ala[4] by a NCDAA. The specificity and toxic mechanism of Tlde1 are different from previously characterized T6SS effectors targeting the peptidoglycan. T6SS amidase effectors Tae1 and Tae4 cleave the bond between D-*i*Glu[2] and *m*DAP[3] within the same peptide stem, while Tae2 and Tae3 cleave the crosslink bridge between D-Ala[4] and *m*DAP[3] of different peptide stems (Russell et al., 2012). T6SS glycoside hydrolases (Tge) cleave the glycoside bond between NAM and NAG (Whitney et al., 2013). In addition, the evolutionary origin of Tlde1 is different from T6SS amidases: while the Tae1–Tae4 catalytic domains are related to CHAP (PF05257) and NlpC/P60 (PF00877) amidases (Anantharaman and Aravind, 2003; Bateman and Rawlings, 2003), the Tlde1a–Tlde1c catalytic domains are related to YkuD of L,D-TPases (PF03734) (Biarrotte-Sorin et al., 2006).

Due to the importance of peptidoglycan in providing shape and resistance to osmotic pressure, it is not surprising that a large number of bacterial toxins target the synthesis and/or integrity of the sacculus. The peptidoglycan is made of glycan strands crosslinked by short peptides, whose composition is highly diverse among bacterial species (Vollmer and Born, 2009). The greatest variation occurs at the third position of the peptide stem, which is *m*DAP in almost all Gram-negative bacteria (including some species of *Bacillus*, *Lactobacilli*, and *Mycobacterium*) and L-Lys in most Gram-positive bacteria, but other amino acids can occur at this position such as L-ornithine, D-Lys, *meso*-lanthionine, L-homoserine, L-Ala and L-Glu. Moreover, *m*DAP and L-Lys can be hydroxylated or amidated in a few species (Vollmer and Born, 2009). Such variability in the peptidoglycan may be the reason why T6SS-containing bacteria use such a diverse array of effectors to target this important structure. A detailed study of 20 species representing 5 orders of the class Alphaproteobacteria revealed a great diversity in peptide stem composition and crosslink (Espaillat et al., 2016). Modifications in the peptidoglycan of Acetobacteria could provide protection against T6SS amidases Tae1 from *Pseudomonas aeruginosa* and Tae2 from *Acidovorax citrulli*; these species naturally coexist in the soil (Espaillat et al., 2016).

Besides the variability in target-cell peptidoglycan structure, it is known that T6SS effectors display conditional toxicity depending on pH, salinity, temperature, and oxygen availability (LaCourse et al., 2018). Furthermore, some effectors exhibit a synergistic effect and are more proficient in killing target cells when combined with other T6SS effectors (LaCourse et al., 2018). This evidence helps explain why bacteria harbor so many effectors for the same cellular target. In the case of *Salmonella enterica*, most serovars live in a variety of environments such as soil, water, plants, and vertebrate hosts (e.g., chicken, cattle, humans) (Bäumler et al., 1998; Winfield and Groisman, 2003). In light of this vast range of environmental conditions, one can only imagine the great diversity of rival bacterial species encountered, so it makes sense for *Salmonella* to deliver a cocktail of effectors into target cells, which may have different levels of effectiveness depending on the pH, salinity, temperature, and oxygen availability at that specific encounter. This could be the case for *Salmonella* Tae4 effector and the newly identified Tlde1.

L,D-TPases form *m*DAP[3]-*m*DAP[3] crosslinks between peptide stems by transferring the peptide bond between the third residue of a tetrapeptide donor stem to the side-chain amide group of a third residue of an adjacent acceptor stem. The catalytic mechanism was proposed to occur in a two-step enzymatic reaction requiring a cysteine residue; it involves the acylation of the enzyme by the penultimate peptide of the donor stem with the release of the C-terminal amino acid residue D-Ala[4], followed by deacylation of this acyl-enzyme intermediate by an acceptor stem (Biarrotte-Sorin et al., 2006; Erdemli et al., 2012). Enzymes displaying L,D-TPase activity (Ldt_{Bs}, Ldt_{fm}, Ldt_{Mt}) (clades 2 and 3; Figure 3A) have an elongated active site, with the catalytic residues accessible via two paths. However, Csd6 from *H. pylori*, which displays an L,D-TPase domain but only L,D-CPase activity (clade 4; Figure 3A), has the active site in a deep pocket, with the catalytic triad positioned at the bottom and accessible via a single narrow path (Kim et al., 2015). The absence of detailed structural information for Tlde1 does not allow us to determine its precise catalytic mechanism at this point; however, we speculate that structural features that restrict access to its active site may explain its activity. The lack of crosslinked GM-tetrapeptide dimer products during *in vitro* assays (Figure 3D) and their L,D-CPase and D-amino acid exchange activities support the hypothesis that the active site of Tlde1 is not accessible to larger acceptor substrates such as GM-tetrapeptides; instead, Tlde1 preferentially uses small molecules such as water and free amino acids as acceptors.

Peptidoglycan synthesis is differentially controlled during cell division and elongation, with the septal synthesis machinery being favored during cell division (Woldringh et al., 1987; Wientjes and Nanninga, 1989). It has been shown that cell division is mediated by the filaments of FtsZ and FtsA that treadmill circumferentially around the division ring and drive the motion of peptidoglycan-synthesizing enzymes (Bisson-Filho et al., 2017; Yang et al., 2017). The rate of division septum closure is mainly determined by the D,D-TPase activity of FtsI (Coltharp et al., 2016). The toxic phenotype induced by periplasmic expression of Tlde1 seems to be the result of a series of events. First, up to 4.5 h of intoxication, cells stop dividing but continue growing in length. Our hypothesis that Tlde1 promotes toxicity by interfering with peptidoglycan synthesis and transpeptidation fits with the finding that division septum closure is limited by peptidoglycan synthesis. Second, the phenotype observed after 4.5 h in which cells form blebs and lyse (Video S2) is also aligned with the idea of diminished peptidoglycan synthesis and crosslink rates; when the peptidoglycan growth rate falls behind that of overall cell growth, the peptidoglycan net stretches, resulting in changes in pore size that alter the integrity of the cell wall (Typas et al., 2011).

In T6SS$^+$ organisms, Tlde1 proteins are encoded in bicistrons with their putative immunity proteins (Figure 4C). Divergence among immunity proteins was considerably higher than that found within the effector families. The immunity protein for Tlde1a subfamily has a DUF2195 domain (Tldi1a), while Tldi1b and Tldi1c immunity proteins are encoded by genes with no annotated domain. Tldi1a and Tldi1b immunity proteins encode a Sec signal peptide for periplasmic localization, while Tldi1c immunity proteins have one or more transmembrane domains

(Figure S1) (Krogh et al., 2001). A similar diversity in localization signals of T6SS immunity proteins was observed for homologs of the toxin encoded at the C-terminal of VgrG2b (DUF4157) of *Pseudomonas aeruginosa* (Wood et al., 2019). The greater sequence divergence in immunity proteins has been reported previously and is likely due to less restrictive selective pressure compared to effectors; while immunity proteins are selected for effector binding, effectors are selected for both immunity protein binding and catalysis (Russell et al., 2012). Due to the small length of these immunity proteins and their diversity, which impeded automated bioinformatic analysis, we did not attempt further assessment of their phylogeny.

T6SSs translocate effectors by decorating the Hcp-VgrG-PAAR puncturing device (Cianfanelli et al., 2016; Jana and Salomon, 2019). Small effector proteins composed of only one toxic domain, such as Tlde1, usually interact with Hcp proteins for secretion as their size favors fitting inside the narrow tube formed by Hcp hexamers (Silverman et al., 2013; Jana and Salomon, 2019). Further supporting this notion, our bioinformatic analysis showed that Tlde1 family members associated with Hcp proteins (Figure 4C). Initial attempts to detect protein-protein interaction between Tlde1a^{STM} and *S.* Typhimurium Hcp1–3 using bacterial two-hybrid and co-immunoprecipitation were unsuccessful.

The distribution of Tlde1a, Tlde1b, and Tlde1c effectors between different organisms gives an idea of how these toxins are used by different species to intoxicate competitors. It is interesting to note that most *S. enterica* subsp. *enterica* serovars encode only a Tlde1a member (e.g., *S.* Typhimurium). According to our analysis, Tlde1b members are mainly represented among species of the Enterobacteriaceae, indicating that Tlde1b/Tldi1b effector/immunity pairs must be a commonly used ammunition in the gut environment. Therefore, it does not seem to be a great competitive advantage for *S.* Typhimurium to keep a Tlde1b effector in its repertoire as many species already living in the gut encode a Tldi1b immunity. Similarly, despite that most *S. enterica* subsp. *enterica* serovars encode only Tlde1a, they frequently encode an orphan Tldi1b immunity, suggesting that although not attacking competitors using Tlde1b, *Salmonella* are protected from the attack of members of the microbiota encoding a Tlde1b effector. Overall, from the perspective of an enteric pathogen that needs to kill competitor species in the gut to colonize the environment, *S. enterica* subsp. *enterica* serovars are well equipped with a Tlde1a member, which is not present in most members of Enterobacteriaceae.

STAR★METHODS

Detailed methods are provided in the online version of this paper and include the following:

- KEY RESOURCES TABLE
- RESOURCE AVAILABILITY
  - Lead Contact
  - Materials Availability
  - Data and Code Availability
- EXPERIMENTAL MODEL AND SUBJECT DETAILS
- METHOD DETAILS
  - Cloning and mutagenesis
  - Growth inhibition assay
  - Subcellular fractionation
  - Microscopy
  - Recombinant protein expression and purification
  - Peptidoglycan purification and enzymatic assays
  - Bioinformatic analysis
- QUANTIFICATION AND STATISTICAL ANALYSES

SUPPLEMENTAL INFORMATION

Supplemental Information can be found online at https://doi.org/10.1016/j.celrep.2020.107813.

ACKNOWLEDGMENTS

We are grateful to Chuck S. Farah (University of São Paulo) for sharing equipment and reagents and for careful reading of this manuscript; Marcelo Brocchi (University of Campinas), Eric Cascales (Aix-Marseille Université), and Alexandre Bisson-Filho (Brandeis University) for bacterial strains; Françoise Norel (Institute Pasteur) and Beny Spira (University of São Paulo) for P22 phage lysate; David Holden (Imperial College London) for antibodies; Mario C. Cruz and Iuri C. Valadão (CEFAP-USP) for support with the microscopy analysis; Gilberto H. Kaihami for assistance with the bioinformatic data collection; and Daniel E.S. Limache for technical support. MS analyses were performed by the Chemistry MS facility at the University of Sheffield. This work was supported by São Paulo Research Foundation (FAPESP) grants to E.B.-S. (2017/02178-2), R.F.d.S. (2016/09047-8), and C.R.G. (2017/17303-7, 2019/00195-2). FAPESP fellowships were awarded to S.S.-S. (2018/13819-1), J.T.H. (2018/25316-4), B.Y.M. (2016/00458-5), and E.B.-S. (2018/04553-8). G.G.N. was awarded a CAPES fellowship. A.P. is supported by a Biotechnology and Biological Sciences Research Council (BBSRC) studentship (BB/M011151/1).

AUTHOR CONTRIBUTIONS

S.S.-S., J.T.H., and E.B.-S. outlined the study. S.S.-S., J.T.H., B.Y.M., and E.B.-S. performed the experiments and analyzed the data. A.P. and S.M. performed the peptidoglycan enzymatic assays and analyzed the data. G.G.N. and R.F.d.S. performed the bioinformatic analyses. S.S.-S., J.T.H., S.M., G.G.N., R.F.d.S., C.R.G., and E.B.-S. contributed to the scientific discussions. S.S.-S. and E.B.-S. wrote the manuscript with input from other authors.

DECLARATION OF INTERESTS

The authors declare no competing interests.

Received: February 17, 2020
Revised: April 20, 2020
Accepted: June 3, 2020
Published: June 23, 2020

REFERENCES

Abby, S.S., Cury, J., Guglielmini, J., Néron, B., Touchon, M., and Rocha, E.P. (2016). Identification of protein secretion systems in bacterial genomes. Sci. Rep. *6*, 23080.

Ahmad, S., Wang, B., Walker, M.D., Tran, H.R., Stogios, P.J., Savchenko, A., Grant, R.A., McArthur, A.G., Laub, M.T., and Whitney, J.C. (2019). An interbacterial toxin inhibits target cell growth by synthesizing (p)ppApp. Nature *575*, 674–678.

Almagro Armenteros, J.J., Tsirigos, K.D., Sønderby, C.K., Petersen, T.N., Winther, O., Brunak, S., von Heijne, G., and Nielsen, H. (2019). SignalP 5.0 improves signal peptide predictions using deep neural networks. Nat. Biotechnol. *37*, 420–423.

Altindis, E., Dong, T., Catalano, C., and Mekalanos, J. (2015). Secretome analysis of *Vibrio cholerae* type VI secretion system reveals a new effector-immunity pair. MBio *6*, e00075.

Anantharaman, V., and Aravind, L. (2003). Evolutionary history, structural features and biochemical diversity of the NlpC/P60 superfamily of enzymes. Genome Biol. *4*, R11.

Bao, H., Zhao, J.H., Zhu, S., Wang, S., Zhang, J., Wang, X.Y., Hua, B., Liu, C., Liu, H., and Liu, S.L. (2019). Genetic diversity and evolutionary features of type VI secretion systems in *Salmonella*. Future Microbiol. *14*, 139–154.

Bateman, A., and Rawlings, N.D. (2003). The CHAP domain: a large family of amidases including GSP amidase and peptidoglycan hydrolases. Trends Biochem. Sci. *28*, 234–237.

Bäumler, A.J., Tsolis, R.M., Ficht, T.A., and Adams, L.G. (1998). Evolution of host adaptation in *Salmonella enterica*. Infect. Immun. *66*, 4579–4587.

Bayer-Santos, E., Cenens, W., Matsuyama, B.Y., Oka, G.U., Di Sessa, G., Mininel, I.D.V., Alves, T.L., and Farah, C.S. (2019). The opportunistic pathogen *Stenotrophomonas maltophilia* utilizes a type IV secretion system for interbacterial killing. PLoS Pathog. *15*, e1007651.

Benz, J., Reinstein, J., and Meinhart, A. (2013). Structural Insights into the Effector - Immunity System Tae4/Tai4 from *Salmonella typhimurium*. PLoS ONE *8*, e67362.

Beraud, M., Kolb, A., Monteil, V., D'Alayer, J., and Norel, F. (2010). A proteomic analysis reveals differential regulation of the σ(S)-dependent yciGFE(katN) locus by YncC and H-NS in Salmonella and Escherichia coli K-12. Mol. Cell. Proteomics *9*, 2601–2616.

Bertsche, U., Breukink, E., Kast, T., and Vollmer, W. (2005). *In vitro* murein peptidoglycan synthesis by dimers of the bifunctional transglycosylase-transpeptidase PBP1B from *Escherichia coli*. J. Biol. Chem. *280*, 38096–38101.

Bianchet, M.A., Pan, Y.H., Basta, L.A.B., Saavedra, H., Lloyd, E.P., Kumar, P., Mattoo, R., Townsend, C.A., and Lamichhane, G. (2017). Structural insight into the inactivation of Mycobacterium tuberculosis non-classical transpeptidase Ldt_{Mt2} by biapenem and tebipenem. BMC Biochem. *18*, 8.

Biarrotte-Sorin, S., Hugonnet, J.E., Delfosse, V., Mainardi, J.L., Gutmann, L., Arthur, M., and Mayer, C. (2006). Crystal structure of a novel beta-lactam-insensitive peptidoglycan transpeptidase. J. Mol. Biol. *359*, 533–538.

Bielnicki, J., Devedjiev, Y., Derewenda, U., Dauter, Z., Joachimiak, A., and Derewenda, Z.S. (2006). *B. subtilis* ykuD protein at 2.0 A resolution: insights into the structure and function of a novel, ubiquitous family of bacterial enzymes. Proteins *62*, 144–151.

Bisson-Filho, A.W., Hsu, Y.P., Squyres, G.R., Kuru, E., Wu, F., Jukes, C., Sun, Y., Dekker, C., Holden, S., VanNieuwenhze, M.S., et al. (2017). Treadmilling by FtsZ filaments drives peptidoglycan synthesis and bacterial cell division. Science *355*, 739–743.

Blondel, C.J., Jiménez, J.C., Contreras, I., and Santiviago, C.A. (2009). Comparative genomic analysis uncovers 3 novel loci encoding type six secretion systems differentially distributed in *Salmonella* serotypes. BMC Genomics *10*, 354.

Born, P., Breukink, E., and Vollmer, W. (2006). *In vitro* synthesis of cross-linked murein and its attachment to sacculi by PBP1A from Escherichia coli. J. Biol. Chem. *281*, 26985–26993.

Brunet, Y.R., Khodr, A., Logger, L., Aussel, L., Mignot, T., Rimsky, S., and Cascales, E. (2015). H-NS Silencing of the *Salmonella* Pathogenicity Island 6-Encoded Type VI Secretion System Limits *Salmonella enterica* Serovar Typhimurium Interbacterial Killing. Infect. Immun. *83*, 2738–2750.

Capella-Gutiérrez, S., Silla-Martínez, J.M., and Gabaldón, T. (2009). trimAl: a tool for automated alignment trimming in large-scale phylogenetic analyses. Bioinformatics *25*, 1972–1973.

Catherwood, A.C., Lloyd, A.J., Tod, J.A., Chauhan, S., Slade, S.E., Walkowiak, G.P., Galley, N.F., Punekar, A.S., Smart, K., Rea, D., et al. (2020). Substrate and Stereochemical Control of Peptidoglycan Cross-Linking by Transpeptidation by *Escherichia coli* PBP1B. J. Am. Chem. Soc. *142*, 5034–5048.

Cava, F., de Pedro, M.A., Lam, H., Davis, B.M., and Waldor, M.K. (2011). Distinct pathways for modification of the bacterial cell wall by non-canonical D-amino acids. EMBO J. *30*, 3442–3453.

Caveney, N.A., Caballero, G., Voedts, H., Niciforovic, A., Worrall, L.J., Vuckovic, M., Fonvielle, M., Hugonnet, J.E., Arthur, M., and Strynadka, N.C.J. (2019). Structural insight into YcbB-mediated beta-lactam resistance in *Escherichia coli*. Nat. Commun. *10*, 1849.

Chen, L., Song, N., Liu, B., Zhang, N., Alikhan, N.F., Zhou, Z., Zhou, Y., Zhou, S., Zheng, D., Chen, M., et al. (2019). Genome-wide Identification and Characterization of a Superfamily of Bacterial Extracellular Contractile Injection Systems. Cell Rep. *29*, 511–521.e2.

Cianfanelli, F.R., Monlezun, L., and Coulthurst, S.J. (2016). Aim, Load, Fire: The Type VI Secretion System, a Bacterial Nanoweapon. Trends Microbiol. *24*, 51–62.

Coltharp, C., Buss, J., Plumer, T.M., and Xiao, J. (2016). Defining the rate-limiting processes of bacterial cytokinesis. Proc. Natl. Acad. Sci. USA *113*, E1044–E1053.

Coulthurst, S. (2019). The Type VI secretion system: a versatile bacterial weapon. Microbiology *165*, 503–515.

Datsenko, K.A., and Wanner, B.L. (2000). One-step inactivation of chromosomal genes in *Escherichia coli* K-12 using PCR products. Proc. Natl. Acad. Sci. USA *97*, 6640–6645.

DeShazer, D. (2019). A novel contact-independent T6SS that maintains redox homeostasis via Zn^{2+} and Mn^{2+} acquisition is conserved in the Burkholderia pseudomallei complex. Microbiol. Res. *226*, 48–54.

Dykxhoorn, D.M., St Pierre, R., and Linn, T. (1996). A set of compatible tac promoter expression vectors. Gene *177*, 133–136.

El-Gebali, S., Mistry, J., Bateman, A., Eddy, S.R., Luciani, A., Potter, S.C., Qureshi, M., Richardson, L.J., Salazar, G.A., Smart, A., et al. (2019). The Pfam protein families database in 2019. Nucleic Acids Res. *47* (*D1*), D427–D432.

English, G., Trunk, K., Rao, V.A., Srikannathasan, V., Hunter, W.N., and Coulthurst, S.J. (2012). New secreted toxins and immunity proteins encoded within the Type VI secretion system gene cluster of *Serratia marcescens*. Mol. Microbiol. *86*, 921–936.

Erdemli, S.B., Gupta, R., Bishai, W.R., Lamichhane, G., Amzel, L.M., and Bianchet, M.A. (2012). Targeting the cell wall of *Mycobacterium tuberculosis*: structure and mechanism of L,D-transpeptidase 2. Structure *20*, 2103–2115.

Espaillat, A., Forsmo, O., El Biari, K., Björk, R., Lemaitre, B., Trygg, J., Cañada, F.J., de Pedro, M.A., and Cava, F. (2016). Chemometric Analysis of Bacterial Peptidoglycan Reveals Atypical Modifications That Empower the Cell Wall against Predatory Enzymes and Fly Innate Immunity. J. Am. Chem. Soc. *138*, 9193–9204.

García-Bayona, L., and Comstock, L.E. (2018). Bacterial antagonism in host-associated microbial communities. Science *361*, eaat2456.

Gauthier, A., Puente, J.L., and Finlay, B.B. (2003). Secretin of the enteropathogenic *Escherichia coli* type III secretion system requires components of the type III apparatus for assembly and localization. Infect. Immun. *71*, 3310–3319.

Glauner, B., Höltje, J.V., and Schwarz, U. (1988). The composition of the murein of *Escherichia coli*. J. Biol. Chem. *263*, 10088–10095.

Hachani, A., Wood, T.E., and Filloux, A. (2016). Type VI secretion and anti-host effectors. Curr. Opin. Microbiol. *29*, 81–93.

Hernandez, S.B., Dorr, T., Waldor, M.K., and Cava, F. (2020). Modulation of Peptidoglycan Synthesis by Recycled Cell Wall Tetrapeptides. Cell Rep. *31*, 107578.

Hood, R.D., Singh, P., Hsu, F., Güvener, T., Carl, M.A., Trinidad, R.R., Silverman, J.M., Ohlson, B.B., Hicks, K.G., Plemel, R.L., et al. (2010). A type VI secretion system of *Pseudomonas aeruginosa* targets a toxin to bacteria. Cell Host Microbe *7*, 25–37.

Jana, B., and Salomon, D. (2019). Type VI secretion system: a modular toolkit for bacterial dominance. Future Microbiol. *14*, 1451–1463.

Jana, B., Fridman, C.M., Bosis, E., and Salomon, D. (2019). A modular effector with a DNase domain and a marker for T6SS substrates. Nat. Commun. *10*, 3595.

Katoh, K., Kuma, K., Toh, H., and Miyata, T. (2005). MAFFT version 5: improvement in accuracy of multiple sequence alignment. Nucleic Acids Res. *33*, 511–518.

Kim, H.S., Im, H.N., An, D.R., Yoon, J.Y., Jang, J.Y., Mobashery, S., Hesek, D., Lee, M., Yoo, J., Cui, M., et al. (2015). The Cell Shape-determining Csd6 Protein from *Helicobacter pylori* Constitutes a New Family of L,D-Carboxypeptidase. J. Biol. Chem. *290*, 25103–25117.

King, D.T., Sobhanifar, S., and Strynadka, N.C. (2016). One ring to rule them all: current trends in combating bacterial resistance to the β-lactams. Protein Sci. *25*, 787–803.

Koskiniemi, S., Lamoureux, J.G., Nikolakakis, K.C., t'Kint de Roodenbeke, C., Kaplan, M.D., Low, D.A., and Hayes, C.S. (2013). Rhs proteins from diverse bacteria mediate intercellular competition. Proc. Natl. Acad. Sci. USA *110*, 7032–7037.

Krogh, A., Larsson, B., von Heijne, G., and Sonnhammer, E.L. (2001). Predicting transmembrane protein topology with a hidden Markov model: application to complete genomes. J. Mol. Biol. *305*, 567–580.

Kumar, P., Chauhan, V., Silva, J.R.A., Lameira, J., d'Andrea, F.B., Li, S.G., Ginell, S.L., Freundlich, J.S., Alves, C.N., Bailey, S., et al. (2017). *Mycobacterium abscessus* l,d-Transpeptidases Are Susceptible to Inactivation by Carbapenems and Cephalosporins but Not Penicillins. Antimicrob. Agents Chemother. *61*, e00866-17.

LaCourse, K.D., Peterson, S.B., Kulasekara, H.D., Radey, M.C., Kim, J., and Mougous, J.D. (2018). Conditional toxicity and synergy drive diversity among antibacterial effectors. Nat. Microbiol. *3*, 440–446.

Lam, H., Oh, D.C., Cava, F., Takacs, C.N., Clardy, J., de Pedro, M.A., and Waldor, M.K. (2009). D-amino acids govern stationary phase cell wall remodeling in bacteria. Science *325*, 1552–1555.

Lucchini, S., Rowley, G., Goldberg, M.D., Hurd, D., Harrison, M., and Hinton, J.C. (2006). H-NS mediates the silencing of laterally acquired genes in bacteria. PLoS Pathog. *2*, e81.

Ma, L.S., Hachani, A., Lin, J.S., Filloux, A., and Lai, E.M. (2014). *Agrobacterium tumefaciens* deploys a superfamily of type VI secretion DNase effectors as weapons for interbacterial competition in planta. Cell Host Microbe *16*, 94–104.

Ma, J., Sun, M., Pan, Z., Lu, C., and Yao, H. (2018). Diverse toxic effectors are harbored by vgrG islands for interbacterial antagonism in type VI secretion system. Biochim. Biophys. Acta, Gen. Subj. *1862*, 1635–1643.

Mainardi, J.L., Fourgeaud, M., Hugonnet, J.E., Dubost, L., Brouard, J.P., Ouazzani, J., Rice, L.B., Gutmann, L., and Arthur, M. (2005). A novel peptidoglycan cross-linking enzyme for a beta-lactam-resistant transpeptidation pathway. J. Biol. Chem. *280*, 38146–38152.

Mariano, G., Trunk, K., Williams, D.J., Monlezun, L., Strahl, H., Pitt, S.J., and Coulthurst, S.J. (2019). A family of Type VI secretion system effector proteins that form ion-selective pores. Nat. Commun. *10*, 5484.

Meberg, B.M., Sailer, F.C., Nelson, D.E., and Young, K.D. (2001). Reconstruction of *Escherichia coli* mrcA (PBP 1a) mutants lacking multiple combinations of penicillin binding proteins. J. Bacteriol. *183*, 6148–6149.

Mesnage, S., Chau, F., Dubost, L., and Arthur, M. (2008). Role of N-acetylglucosaminidase and N-acetylmuramidase activities in *Enterococcus faecalis* peptidoglycan metabolism. J. Biol. Chem. *283*, 19845–19853.

Moore, D.A., Whatley, Z.N., Joshi, C.P., Osawa, M., and Erickson, H.P. (2016). Probing for Binding Regions of the FtsZ Protein Surface through Site-Directed Insertions: Discovery of Fully Functional FtsZ-Fluorescent Proteins. J. Bacteriol. *199*, e00553-16.

Mougous, J.D., Cuff, M.E., Raunser, S., Shen, A., Zhou, M., Gifford, C.A., Goodman, A.L., Joachimiak, G., Ordoñez, C.L., Lory, S., et al. (2006). A virulence locus of *Pseudomonas aeruginosa* encodes a protein secretion apparatus. Science *312*, 1526–1530.

Mulder, D.T., Cooper, C.A., and Coombes, B.K. (2012). Type VI secretion system-associated gene clusters contribute to pathogenesis of *Salmonella enterica* serovar Typhimurium. Infect. Immun. *80*, 1996–2007.

Navarre, W.W., Porwollik, S., Wang, Y., McClelland, M., Rosen, H., Libby, S.J., and Fang, F.C. (2006). Selective silencing of foreign DNA with low GC content by the H-NS protein in *Salmonella*. Science *313*, 236–238.

Nguyen, V.S., Douzi, B., Durand, E., Roussel, A., Cascales, E., and Cambillau, C. (2018). Towards a complete structural deciphering of Type VI secretion system. Curr. Opin. Struct. Biol. *49*, 77–84.

Parsons, D.A., and Heffron, F. (2005). sciS, an icmF homolog in *Salmonella enterica* serovar Typhimurium, limits intracellular replication and decreases virulence. Infect. Immun. *73*, 4338–4345.

Potter, S.C., Luciani, A., Eddy, S.R., Park, Y., Lopez, R., and Finn, R.D. (2018). HMMER web server: 2018 update. Nucleic Acids Res. *46* (*W1*), W200–W204.

Price, M.N., Dehal, P.S., and Arkin, A.P. (2010). FastTree 2–approximately maximum-likelihood trees for large alignments. PLOS ONE *5*, e9490.

Renault, M.G., Zamarreno Beas, J., Douzi, B., Chabalier, M., Zoued, A., Brunet, Y.R., Cambillau, C., Journet, L., and Cascales, E. (2018). The gp27-like Hub of VgrG Serves as Adaptor to Promote Hcp Tube Assembly. J. Mol. Biol. *430* (*18 Pt B*), 3143–3156.

Rodríguez-Rubio, L., Gerstmans, H., Thorpe, S., Mesnage, S., Lavigne, R., and Briers, Y. (2016). DUF3380 Domain from a *Salmonella* Phage Endolysin Shows Potent N-Acetylmuramidase Activity. Appl. Environ. Microbiol. *82*, 4975–4981.

Russell, A.B., Hood, R.D., Bui, N.K., LeRoux, M., Vollmer, W., and Mougous, J.D. (2011). Type VI secretion delivers bacteriolytic effectors to target cells. Nature *475*, 343–347.

Russell, A.B., Singh, P., Brittnacher, M., Bui, N.K., Hood, R.D., Carl, M.A., Agnello, D.M., Schwarz, S., Goodlett, D.R., Vollmer, W., and Mougous, J.D. (2012). A widespread bacterial type VI secretion effector superfamily identified using a heuristic approach. Cell Host Microbe *11*, 538–549.

Salih, O., He, S., Planamente, S., Stach, L., Macdonald, J.T., Manoli, E., Scheres, S.H.W., Filloux, A., and Freemont, P.S. (2018). Atomic Structure of Type VI Contractile Sheath from Pseudomonas aeruginosa. Structure *26*, 329–336.e3.

Sana, T.G., Flaugnatti, N., Lugo, K.A., Lam, L.H., Jacobson, A., Baylot, V., Durand, E., Journet, L., Cascales, E., and Monack, D.M. (2016). *Salmonella* Typhimurium utilizes a T6SS-mediated antibacterial weapon to establish in the host gut. Proc. Natl. Acad. Sci. USA *113*, E5044–E5051.

Schindelin, J., Arganda-Carreras, I., Frise, E., Kaynig, V., Longair, M., Pietzsch, T., Preibisch, S., Rueden, C., Saalfeld, S., Schmid, B., et al. (2012). Fiji: an open-source platform for biological-image analysis. Nat. Methods *9*, 676–682.

Shneider, M.M., Buth, S.A., Ho, B.T., Basler, M., Mekalanos, J.J., and Leiman, P.G. (2013). PAAR-repeat proteins sharpen and diversify the type VI secretion system spike. Nature *500*, 350–353.

Si, M., Wang, Y., Zhang, B., Zhao, C., Kang, Y., Bai, H., Wei, D., Zhu, L., Zhang, L., Dong, T.G., and Shen, X. (2017a). The Type VI Secretion System Engages a Redox-Regulated Dual-Functional Heme Transporter for Zinc Acquisition. Cell Rep. *20*, 949–959.

Si, M., Zhao, C., Burkinshaw, B., Zhang, B., Wei, D., Wang, Y., Dong, T.G., and Shen, X. (2017b). Manganese scavenging and oxidative stress response mediated by type VI secretion system in *Burkholderia thailandensis*. Proc. Natl. Acad. Sci. USA *114*, E2233–E2242.

Silverman, J.M., Agnello, D.M., Zheng, H., Andrews, B.T., Li, M., Catalano, C.E., Gonen, T., and Mougous, J.D. (2013). Haemolysin coregulated protein is an exported receptor and chaperone of type VI secretion substrates. Mol. Cell *51*, 584–593.

Souza, D.P., Oka, G.U., Alvarez-Martinez, C.E., Bisson-Filho, A.W., Dunger, G., Hobeika, L., Cavalcante, N.S., Alegria, M.C., Barbosa, L.R.S., Salinas, R.K., Guzzo, C.R., and Farah, C.S. (2015). Bacterial killing via a type IV secretion system. Nat. Commun *6*, 6453.

Steinegger, M., and Söding, J. (2017). MMseqs2 enables sensitive protein sequence searching for the analysis of massive data sets. Nat. Biotechnol. *35*, 1026–1028.

Tang, J.Y., Bullen, N.P., Ahmad, S., and Whitney, J.C. (2018). Diverse NADase effector families mediate interbacterial antagonism via the type VI secretion system. J. Biol. Chem. *293*, 1504–1514.

Templin, M.F., Ursinus, A., and Höltje, J.V. (1999). A defect in cell wall recycling triggers autolysis during the stationary growth phase of Escherichia coli. EMBO J. *18*, 4108–4117.

Ting, S.Y., Bosch, D.E., Mangiameli, S.M., Radey, M.C., Huang, S., Park, Y.J., Kelly, K.A., Filip, S.K., Goo, Y.A., Eng, J.K., et al. (2018). Bifunctional Immunity Proteins Protect Bacteria against FtsZ-Targeting ADP-Ribosylating Toxins. Cell *175*, 1380–1392.e14.

Trunk, K., Coulthurst, S.J., and Quinn, J. (2019). A New Front in Microbial Warfare-Delivery of Antifungal Effectors by the Type VI Secretion System. J. Fungi (Basel) *5*, 50.

Typas, A., Banzhaf, M., Gross, C.A., and Vollmer, W. (2011). From the regulation of peptidoglycan synthesis to bacterial growth and morphology. Nat. Rev. Microbiol. *10*, 123–136.

Vollmer, W., and Bertsche, U. (2008). Murein (peptidoglycan) structure, architecture and biosynthesis in *Escherichia coli*. Biochim. Biophys. Acta *1778*, 1714–1734.

Vollmer, W., and Born, P. (2009). Bacterial Cell Envelope Peptidoglycan (Elsevier).

Vollmer, W., Blanot, D., and de Pedro, M.A. (2008). Peptidoglycan structure and architecture. FEMS Microbiol. Rev. *32*, 149–167.

Wang, T., Si, M., Song, Y., Zhu, W., Gao, F., Wang, Y., Zhang, L., Zhang, W., Wei, G., Luo, Z.Q., and Shen, X. (2015). Type VI Secretion System Transports Zn2+ to Combat Multiple Stresses and Host Immunity. PLoS Pathog. *11*, e1005020.

Wang, J., Brackmann, M., Castaño-Díez, D., Kudryashev, M., Goldie, K.N., Maier, T., Stahlberg, H., and Basler, M. (2017). Cryo-EM structure of the extended type VI secretion system sheath-tube complex. Nat. Microbiol. *2*, 1507–1512.

Wang, J., Yang, B., Leier, A., Marquez-Lago, T.T., Hayashida, M., Rocker, A., Zhang, Y., Akutsu, T., Chou, K.C., Strugnell, R.A., et al. (2018). Bastion6: a bioinformatics approach for accurate prediction of type VI secreted effectors. Bioinformatics *34*, 2546–2555.

Wang, S., Yang, D., Wu, X., Yi, Z., Wang, Y., Xin, S., Wang, D., Tian, M., Li, T., Qi, J., et al. (2019). The Ferric Uptake Regulator Represses Type VI Secretion System Function by Binding Directly to the *clpV* Promoter in *Salmonella enterica* Serovar Typhimurium. Infect. Immun. *87*, e00562-19.

Whitney, J.C., Chou, S., Russell, A.B., Biboy, J., Gardiner, T.E., Ferrin, M.A., Brittnacher, M., Vollmer, W., and Mougous, J.D. (2013). Identification, structure, and function of a novel type VI secretion peptidoglycan glycoside hydrolase effector-immunity pair. J. Biol. Chem. *288*, 26616–26624.

Wientjes, F.B., and Nanninga, N. (1989). Rate and topography of peptidoglycan synthesis during cell division in *Escherichia coli*: concept of a leading edge. J. Bacteriol. *171*, 3412–3419.

Winfield, M.D., and Groisman, E.A. (2003). Role of nonhost environments in the lifestyles of *Salmonella* and *Escherichia coli*. Appl. Environ. Microbiol. *69*, 3687–3694.

Woldringh, C.L., Huls, P., Pas, E., Brakenhoff, G.J., and Nanninga, N. (1987). Topography of Peptidoglycan Synthesis during Elongation and Polar Cap Formation in a Cell Division Mutant of *Escherichia coli* MC4100. Microbiology *133*, 575–586.

Wood, T.E., Howard, S.A., Forster, A., Nolan, L.M., Manoli, E., Bullen, N.P., Yau, H.C.L., Hachani, A., Hayward, R.D., Whitney, J.C., et al. (2019). The Pseudomonas aeruginosa T6SS Delivers a Periplasmic Toxin that Disrupts Bacterial Cell Morphology. Cell Rep. *29*, 187–201.e7.

Yang, X., Lyu, Z., Miguel, A., McQuillen, R., Huang, K.C., and Xiao, J. (2017). GTPase activity-coupled treadmilling of the bacterial tubulin FtsZ organizes septal cell wall synthesis. Science *355*, 744–747.

Zhang, D., de Souza, R.F., Anantharaman, V., Iyer, L.M., and Aravind, L. (2012). Polymorphic toxin systems: Comprehensive characterization of trafficking modes, processing, mechanisms of action, immunity and ecology using comparative genomics. Biol. Direct *7*, 18.

Zhang, H., Zhang, H., Gao, Z.Q., Wang, W.J., Liu, G.F., Xu, J.H., Su, X.D., and Dong, Y.H. (2013). Structure of the type VI effector-immunity complex (Tae4-Tai4) provides novel insights into the inhibition mechanism of the effector by its immunity protein. J. Biol. Chem. *288*, 5928–5939.

STAR★METHODS

KEY RESOURCES TABLE

REAGENT or RESOURCE	SOURCE	IDENTIFIER
Antibodies		
Rabbit polyclonal anti-FLAG	Sigma-Aldrich	Cat#F7425
Mouse monoclonal anti-DNAk	Abcam	Cat#ab69617
Mouse monoclonal anti-maltose binding protein (MBP)	New England BioLabs	Cat#E8032L
Rabbit polyclonal anti-outer membrane protein A (OmpA)	David Holden	N/A
Bacterial and Virus Strains		
Salmonella Typhimurium str. 14028s wild-type	Marcelo Brocchi	ATCC 14028
S. Typhimurium str. LT2 wild-type	Eric Cascales	ATCC 700720
S. Typhimurium str. LT2 Δ*tssL* (STM0282)	This paper	N/A
S. Typhimurium str. LT2 Δ*tlde1/tldi1* (STM0287/0288)	This paper	N/A
S. Typhimurium str. LT2 Δ*hns* (STM1751)	This paper	N/A
Escherichia coli DH5α	Lab Stock	N/A
E. coli SHuffle T7	New England Biolabs	Cat#C3026J
E. coli XL10-Gold	Agilent Technologies	Cat#200314
E. coli BW27783 strain ftsZ::ftsZ-mVenus	Moore et al., 2016	N/A
E. coli Δ*6ldt*	Meberg et al., 2001	N/A
P22 phage lysate Δ*hns*	Beraud et al., 2010	N/A
Chemicals, Peptides, and Recombinant Proteins		
FM4-64	Molecular Probes	Cat#T3166
Pronase	Roche	Cat#10 165 921 001
Mutanolysin	Sigma-Aldrich	Cat#M9901
Critical Commercial Assays		
QuikChange II XL Site-Directed Mutagenesis Kit	Agilent Technologies	Cat#200521
Oligonucleotides		
See Table S3 for full list.	N/A	N/A
Recombinant DNA		
pKD46	Datsenko and Wanner, 2000	N/A
pKD4	Datsenko and Wanner, 2000	N/A
pCP20	Datsenko and Wanner, 2000	N/A
pBRA	Souza et al., 2015	N/A
pBRA-SP	Bayer-Santos et al., 2019	N/A
pBRA Tlde1	This paper	N/A
pBRA SP-Tlde1	This paper	N/A
pBRA SP-Tlde1(H121A)	This paper	N/A
pBRA SP-Tlde1(C131A)	This paper	N/A
pEXT22	Dykxhoorn et al., 1996	N/A
pEXT22 Tldi1a	This paper	N/A
pEXT22 Tldi1a-FLAG	This paper	N/A
pEXT22 Tldi1b	This paper	N/A
pET28a	Novagen	Cat#69864-3
pET28a-Tlde1	This paper	N/A

(*Continued on next page*)

Continued

REAGENT or RESOURCE	SOURCE	IDENTIFIER
Software and Algorithms		
Neighborhood script	Robson F. de Souza	upon request
MassHunter	Agilent Technologies	N/A
FIJI	Schindelin et al., 2012	https://fiji.sc/
MMseqs	Steinegger and Söding, 2017	https://search.mmseqs.com/search
FastTree 2	Price et al., 2010	http://www.microbesonline.org/fasttree/

RESOURCE AVAILABILITY

Lead Contact

Further information and requests for reagents should be directed to and will be fulfilled by the Lead Contact, Ethel Bayer Santos (ebayersantos@usp.br).

Materials Availability

Strains and plasmids generated in this study are available upon request to the Lead Contact, Ethel Bayer Santos (ebayersantos@usp.br).

Data and Code Availability

The code for data collection and analysis of gene neighborhood used in this study is available upon request to the Lead Contact, Ethel Bayer Santos (ebayersantos@usp.br).

EXPERIMENTAL MODEL AND SUBJECT DETAILS

A list of bacterial strains used in this work can be found in Key Resources Table. Strains were grown at 37°C in Lysogeny Broth (10 g/L tryptone, 10 g/L NaCl, 5 g/L yeast extract) under agitation. Cultures were supplemented with antibiotics in the following concentration when necessary: 50 μg/mL kanamycin, 100 μg/mL ampicillin, 50 μg/mL streptomycin, 15 μg/mL chloramphenicol.

METHOD DETAILS

Cloning and mutagenesis

S. Typhimurium mutant strains were constructed by λ-Red recombination engineering using a one-step inactivation procedure (Datsenko and Wanner, 2000). All primers are listed in Table S3. *STM14_0336* was amplified by PCR and cloned into pBRA vector under the control of P_{BAD} promoter (Souza et al., 2015) with or without PelB signal peptide sequence from pET22b (Novagen) (Bayer-Santos et al., 2019). Immunity proteins (*STM14_0332* and *STM14_0335*) were cloned into pEXT22 under the control of P_{TAC} promoter (Dykxhoorn et al., 1996). For protein expression and purification, STM14_0336 residues between 2-174 were cloned into pET28a (Novagen), including a N-terminal His-tag. Point mutations were created using QuikChange II XL Site-Directed Mutagenesis Kit (Agilent Technologies) and pBRA SP-Tlde1 plasmid was used as template. All constructs were confirmed by sequencing.

Growth inhibition assay

Overnight cultures of *E. coli* DH5α co-expressing effectors for cytoplasmic (pBRA-Tlde1) or periplasmic (pBRA SP-Tlde1) localization and immunity proteins (pEXT22-Tldi1) were serially diluted in LB (1:4) and 5 μL were spotted onto LB agar (1.5%) containing either 0.2% D-glucose or 0.2% L-arabinose and 200 μM IPTG plus streptomycin and kanamycin and incubated at 37°C. Images were acquired after 24h.

Bacterial competition assays were performed using *S.* Typhimurium LT2 strain (WT, Δ*tssL* and Δ*tlde1/tldi1*) either in the Δ*hns* (activated T6SS) or WT background (repressed T6SS). LT2 strain has a point mutation in *rpoS* gene which helps support the detrimental effect of *hns* deletion (Navarre et al., 2006; Lucchini et al., 2006). Due to the high frequency of spontaneous compensatory mutations, Δ*hns* strains were freshly prepared at every experiment by P22 phage transduction (Beraud et al., 2010). Overnight cultures of attacker and prey cells were subculture (1:10) until reaching OD_{600nm} 1, cultures were mixed 4:1 attacker:prey (OD_{600nm} 0.5), 5 μL spotted onto 0.22 μm nitrocellulose membranes (1 × 1 cm), and incubated on LB agar for 16 h at 30°C. The membranes containing the bacterial mixture was placed on 1.5 mL tubes containing 1 mL LB, homogenized by vortex, serially diluted, and plated on selective plates with antibiotics. Prey recovery rate was calculated by dividing the CFU counts of the output by the input. Data represent the mean ± SD of three independent experiments performed in triplicate and were analyzed through comparison with WT that were normalized to 1.

Subcellular fractionation

Subcellular fractionation was adapted from Gauthier et al. (2003) and English et al. (2012) and is based on osmotic shock and ultracentrifugation. Briefly, *E. coli* cells harboring pEXT22-Tldi1-FLAG grown overnight with 200 μM of IPTG were harvested (aliquot corresponding to total proteins was collected for analysis), washed twice with phosphate buffer saline (PBS) and resuspended in 1 mL of 50 mM Tris-HCl pH 7.4, 20% sucrose, 10 mM EDTA and protease inhibitor. Cells were incubated for 10 min at 30°C and recovered by centrifugation (10 min, 8000 *g*, 22°C). Pellets were resuspended in 1 mL of ice-cold water and incubated for 10 min on ice. After centrifugation (10 min, 8000 *g*, 4°C), 900 μL of the supernatant was retained for analysis (enriched in periplasmic proteins). The pellet containing cytoplasmic and membrane proteins was resuspended in 1 mL of sonication buffer (10 mM Tris-HCl pH 7 and protease inhibitor), sonicated 6 rounds of 15 s with amplitude 30% and centrifuged (15 min, 16000 *g*, 4°C) to remove insoluble proteins. Supernatant was transferred to an ultracentrifuge tube and centrifugated (1 h, 50000 *g,* 4°C). Supernatant (900 μL) corresponding to the cytoplasmic fraction was retained for analysis, and the pellet with total membrane proteins was washed with sonication buffer once, centrifugated (1 h, 50000 *g*, 4°C) and resuspended in SDS-PAGE buffer. Fractions were precipitated with 4 volumes of acetone and resuspended in equivalent volumes of SDS-PAGE buffer. Protein extracts were separated by SDS-PAGE and analyzed by western blot with anti-FLAG (Sigma-Aldrich #F7425), anti-DNAk (Abcam #ab69617), anti-maltose binding protein (MPB) (New England BioLabs #E8032L) and anti-outer membrane protein (OmpA) antibodies.

Microscopy

For time-lapse microscopy, LB agar pads were prepared by cutting a rectangular piece out of a double-sided adhesive tape which was taped onto a microscopy slide as described previously (Bayer-Santos et al., 2019). *E. coli* DH5α harboring pBRA SP-Tlde1 was spotted onto 1.5% LB agar pads supplemented either with 0.2% D-glucose or 0.2% L-arabinose and antibiotics. Phase contrast images were taken every 15 min for 24 h using a Zeiss AxioVert.Z1 microscope fitted with an AxioCam MRm camera and an α Plan-Apochromat 63x oil objective. Images were analyzed using FIJI software (Schindelin et al., 2012). To quantify the percentage of dividing or non-dividing cells and the cell doubling time, approximately 100 cells were analyzed in each condition. To determine cell length, approximately 30 cells were measured at each time point (from 30 min to 4.5 h), totaling 150 measurements. To visualize membrane labeling, overnight cultures of *E. coli* carrying pBRA SP-Tlde1 were harvested by centrifugation (3 min, 8000 *g*), washed twice with LB and normalized to OD_{600nm} 0.5. Membrane dye FM 4-64 (Molecular Probes) were mixed to cells at 1:1 and 4 μL were spotted onto 1.5% LB agarose pads supplemented with 0.2% D-glucose or 0.2% L-arabinose. After 20 h, cells were imaged using a Zeiss AxioVert.A1 microscope fitted with an AxioCam ICm1 camera and a FLUAR 100x oil objective. To analyze FtsZ localization, overnight cultures of *E. coli* FtsZ-mVenus expressing pBRA SP-Tlde1 were diluted 1:100 and grown in liquid LB media to an OD_{600nm} 0.2. Cells were harvested by centrifugation (3 min, 8000 *g*), washed twice with LB and added 0.2% D-glucose or 0.2% L-arabinose. At OD_{600nm} 0.5 cells were harvested, washed twice with PBS and 4 μL were spotted onto 1.5% PBS agarose pads supplemented with 0.2% D-glucose or 0.2% L-arabinose. Cells were imaged using a Zeiss AxioVert.A1 microscope fitted with an AxioCam ICm1 camera.

Recombinant protein expression and purification

E. coli SHuffle cells expressing pET28a-Tlde1 were subcultured in LB and grown at 37°C to OD_{600nm} 0.7 prior to induction with 0.4 mM IPTG for 16 h at 16°C (150 rpm). Cells were harvested by centrifugation, resuspended with buffer (20 mM Tris-HCl pH 7.35, 200 mM NaCl) and lysed by 10 passages in a French Press system. The lysate soluble fraction was loaded onto a 5 mL HiTrap chelating HP column (GE Healthcare) immobilized with 100 mM cobalt chloride and equilibrated with the lysis buffer. After the removal of unbound proteins, the fusion protein was eluted with lysis buffer supplemented with 400 mM imidazole. Purified proteins were concentrated in Amicon Filter Units (Millipore) before purification by size exclusion chromatography using a HiLoad 26/600 Superdex 75 column (GE Healthcare).

Peptidoglycan purification and enzymatic assays

Peptidoglycan was purified as described by Mesnage et al. (2008) with small modifications. Briefly, bacterial cells were grown in 1 L of LB to OD_{600nm} 0.7 and harvested by centrifugation (15 min, 4000 *g*, 15°C). Pellets were washed with PBS and resuspended in 20 mL of PBS. Cell suspensions were added dropwise to a glass flask containing 80 mL of boiling 5% SDS and incubated for 30 min. Lysates were washed 4 times with water and treated with pronase 2 mg/mL overnight at 60°C. The following day, 1% SDS was added, incubated for 10 min at 95°C and washed 4 times with water. Muropeptides were obtained by digestion with mutanolysin, followed by reduction with sodium borohydride in borate buffer and separation in reverse-phase high performance liquid chromatography (RP-HPLC) (Mesnage et al., 2008). Monomeric and dimeric substrates were purified from reduced disaccharide-peptides obtained from the *E. coli* Δ6*ldt* mutant (Meberg et al., 2001). Briefly, peptidoglycan was digested by mutanolysin and muropeptides reduced prior to their separation by RP-HPLC using a water-acetonitrile gradient. The fragments corresponding to the monomer GM-tetrapeptide and dimer GM-tetrapeptide-GM-tetrapeptide were collected and freeze-dried, later their concentrations were estimated by nuclear magnetic resonance (NMR) using trimethylsilylpropanoic acid (TSP) as a reference. For *in vitro* assays, 10 μM of purified recombinant Tlde1 protein was added to 100 μM of monomeric or dimeric GM-tetrapeptide in buffer containing 50 mM Tris pH 7.5 and 50 mM NaCl and incubated for 4 h at 37°C. Digestion products were analyzed by RP-HPLC-MS as described previously (Rodríguez-Rubio et al., 2016). For the amino acid exchange assay, reactions were performed in the same conditions with the addition

of 1 mM D-methionine. For the muropeptide profile analysis, *E. coli* carrying empty pBRA, pBRA SP-Tlde1 and pBRA SP-Tlde1$_{C131A}$ were used. Cells were grown overnight, subcultured 1:100 in 250 mL of LB and grown until OD_{600nm} 0.5 with 50 μg/mL streptomycin and 0.2% D-glucose. Cells were washed twice with 20 mL of LB, added 0.2% L-arabinose and incubated for 3 h until peptidoglycan was extracted as described above. MS data were analyzed with MassHunter software (Agilent Technologies).

Bioinformatic analysis

Iterative profile searches using JackHMMER (Potter et al., 2018) with a cutoff e-value of 10^{-6} and a maximum of twenty iteration were performed to search for similar sequences in the non-redundant (nr) protein database from the National Center for Biotechnology Information (NCBI). Similarity-based clustering of proteins was carried out using MMseqs software (Steinegger and Söding, 2017). Sequences alignments were produced with MAFFT local-pair algorithm (Katoh et al., 2005) and non-informative columns were removed with trimAl software (Capella-Gutiérrez et al., 2009). Approximately-maximum-likelihood phylogenetic tree were built using FastTree 2 (Price et al., 2010). Proteins were annotated using the Pfam database (El-Gebali et al., 2019) and protein secretion systems were identified using models from TXSSdb (Abby et al., 2016) and the HMMER package (Potter et al., 2018). To collect the neighborhood of the genes of interest an in-house python script was used based on information downloaded from the complete genomes and nucleotide sections of the NCBI database.

QUANTIFICATION AND STATISTICAL ANALYSES

Statistical tests, number of events quantified, standard deviation of the mean, and statistical significance is reported in figure legends. Statistical analysis has been performed using GraphPad Prism5 software and statistical significance is determined by the value of $p < 0.05$.